





39 particularly for Pampas and Pantanal. Customizing variable selection and fire categories based  
40 on biome characteristics could contribute to a more biome-focused and contextually relevant  
41 analysis. Moreover, prioritizing regional-scale analysis is essential for decision-makers and fire  
42 management strategies. FLAME is easily adaptable to be used in various locations and periods,  
43 serving as a valuable tool for more informed and effective fire prevention measures.

44

45 Keywords: Burned Area. Brazilian biomes. Maximum Entropy. Bayesian Inference. Climate.  
46 Fragmentation. Land Use.

47

48

## 49 **1 INTRODUCTION**

50

51 The complexity of the interactions and feedbacks between fire, climate, people, and other earth  
52 system components makes it challenging to be highly confident about what drives fires in  
53 specific locations. Various methods assess the drivers of historical fire events. Some studies  
54 correlate individual drivers with burned area but overlook the interaction of multiple factors  
55 (ANDELA et al., 2017; BARBOSA et al., 2019). Fire Danger Indices capture simultaneous  
56 drivers to gauge fire risk. However, they overlook human-driven ignition causes  
57 (ZACHARAKIS; TSIHRINTZIS, 2023) and typically fail to capture the impact of fuel  
58 availability on burning (KELLEY; HARRISON, 2014). Fire-enabled Land Surface Models  
59 account for these drivers, simulating observable fire regime measures. However, they often  
60 lack accuracy for year-to-year fire patterns and required accuracy to determine fire drivers  
61 (FORKEL et al. 2019) and the causes of individual fire seasons (HANTSON et al., 2020).  
62 Quantifying uncertainty is critical for assigning fire drivers because it allows for a more  
63 accurate assessment of the confidence in our predictions and helps identify the most influential  
64 factors under varying conditions. In this sense, research applying the Maximum Entropy  
65 framework combined with Bayesian Inference can address these gaps.

66

67 The Principle of Maximum Entropy (MaxEnt) states that when trying to estimate the  
68 probability of an event and the information is limited, you should opt for the distribution that  
69 preserves the greatest amount of uncertainty (i.e., maximizes entropy) while still adhering to  
70 your given constraints (PENFIELD, 2003). These constraints reflect prior knowledge about the  
71 probability distribution of a phenomenon of interest (i.e., burned area) based on its relationship  
72 with independent variables. This approach ensures you do not introduce extra assumptions or  
73 biases into your calculations. MaxEnt has its roots in statistical mechanics (JAYNES, 1957).



74 However, the use of its concept in a species distribution model (PHILLIPS et al., 2006)  
75 popularized the approach in several other study areas, including ecology, geophysics, and fires  
76 (JIN et al., 2020; LI et al., 2019; FONSECA et al., 2017). Incorporating Bayesian Inference  
77 alongside the MaxEnt framework further enhances this approach. Bayesian techniques  
78 integrate prior knowledge and observed data to continuously refine the estimation of  
79 uncertainty in the influence of drivers on fire, thereby improving the confidence in a  
80 relationship we find. By leveraging both MaxEnt and Bayesian Inference, we can develop more  
81 robust models that account for the complex and dynamic nature of fire regimes.

82

83 The MaxEnt species distribution model estimates the probability of target presence for given  
84 local conditions (PHILLIPS et al., 2006). Unlike many traditional models, MaxEnt makes  
85 minimal assumptions about the relationships between variables, making it more flexible and  
86 adaptable to complex ecological interactions. Rather than estimating a single value, MaxEnt  
87 models a full probability distribution (ELITH et al., 2011), providing a comprehensive view of  
88 potential outcomes. This probabilistic nature enables the incorporation of prior information  
89 into the modeling process, enhancing its accuracy. Additionally, MaxEnt enables the  
90 quantification of uncertainties (CHEN et al., 2019), providing valuable insights into the  
91 reliability and confidence of model predictions.

92

93 Recognizing that fires can be treated as a species due to their strong dependence on  
94 environmental factors, utilizing the MaxEnt species model has yielded valuable insights into  
95 the field (FERREIRA et al., 2023; FONSECA et al., 2019). However, the MaxEnt model relies  
96 on presence-only or presence/absence data, which means it primarily considers locations where  
97 the target (in this case, fires) has occurred. This limits fire research using MaxEnt as it does not  
98 allow continuous data, such as burned area fraction over a larger region. Moreover, the  
99 constraints and structure of the underlying model are fundamentally related to species  
100 distributions (PHILLIPS et al., 2006) rather than fires, which may not capture the nuances of  
101 fire behavior.

102

103 The simulation of fires in heterogeneous territories such as Brazil is incredibly challenging.  
104 Wildfires have become a pressing concern in the country, causing significant socioeconomic  
105 and environmental losses (CAMPANHARO et al., 2019; BARBOSA et al., 2022; WU et al.,  
106 2023). Since 1980, more than 1,857,025 km<sup>2</sup> of Brazil's terrain has been negatively impacted  
107 by fires (MAPBIOMAS, 2023), reflecting a need for effective and adaptive fire management



108 strategies. Nonetheless, quantifying the influence of these drivers can be difficult - many  
109 interactions between fire and its drivers are non-linear, and drivers heavily interact with each  
110 other, making confidently identifying drivers of fire regimes in such diverse landscapes tricky  
111 from observations alone (KRAWCHUK and MORITZ 2014). While traditional fire models  
112 provide useful broadscale information on fire, land, and climate interactions, they do not  
113 quantify the uncertainty in these relationships and rely on other studies to infer relationships  
114 between drivers and burning (HANTSON et al., 2016).

115

116 Improving fire simulations and understanding the underlying drivers of fires in Brazil is  
117 essential to address the challenges associated with preventing fires, firefighting, and managing  
118 their aftermath. Here, we present and evaluate a novel fire model, FLAME (Fire Landscape  
119 Analysis using Maximum Entropy), based on a Bayesian inference implementation of the  
120 MaxEnt concept. This combination allows us to incorporate uncertainty and probabilistic  
121 reasoning into fire modeling. In this sense, the model aims to precisely measure uncertainties  
122 of the simulations. The model optimizes key driving variables relationship with fires. Here we  
123 apply FLAME to the biomes in Brazil, and assess the performance against observations.

124

## 125 **2 METHODS**

126

### 127 **2.1 Datasets and preprocessing**

128

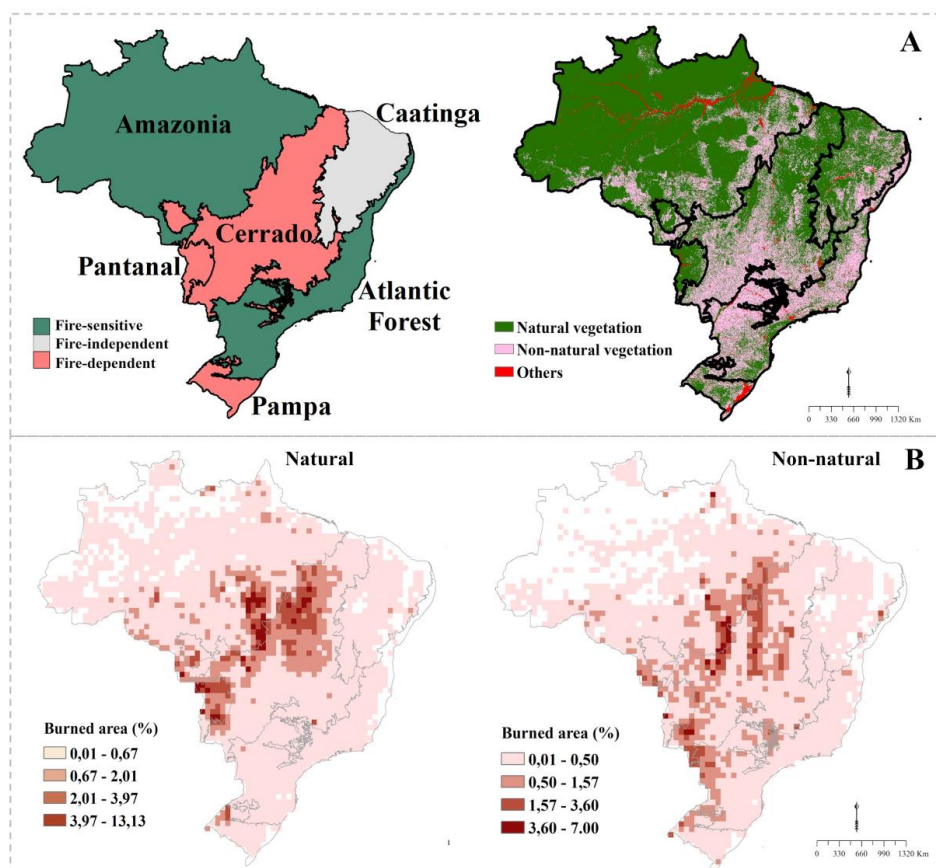
129 We used the MCD64A1 burned area product from MODIS collection 6 as our target variable  
130 (GIGLIO et al., 2018). This data was regridded from 500m to 0.5° spatial resolution. The burned  
131 area data was used in its totality (ALL) and divided into two other categories based on the  
132 LULC data from the Mapbiomas project (<https://brasil.mapbiomas.org/en/>): fires reaching  
133 natural vegetation (NAT) and fires reaching non-natural vegetation (NON) (Fig. 1).

134

135 We computed all burned areas within forests, grasslands, and savannas for the NAT and the  
136 NON within pasture, cropland, and forest plantation, aggregated with croplands. The  
137 categorization of fires aims to assess whether there are distinct drivers for NAT and NON and  
138 to exemplify the potentialities of the model for assessing more than one fire category across  
139 different vegetation types. Amazonia and Atlantic Forest are fire-sensitive biomes (Fig. 1) that  
140 are highly susceptible to damage or destruction by fire. Cerrado, Pampa and Pantanal have



141 evolved to depend on fire as part of their life cycle and are considered fire-dependent biomes.  
142 Finally, Caatinga is a fire-independent biome that is generally not significantly affected by fire  
143 or does not require fire as part of its vegetation dynamics. This categorization follows Hardesty  
144 et al. (2005), based on the predominant vegetation type that defines the biome. However, all  
145 biomes contain vegetation types with different sensitivities to fire. We adopt a broad approach  
146 to encompass the various biomes in Brazil; however, any type of categorization is permissible,  
147 and further studies could focus on even finer stratification, e.g. fires reaching fire-sensitive  
148 vegetation and fire-dependent vegetation within each biome.  
149



150

151 **Figure 1: (A) Brazilian biomes classified as Fire-sensitive, Fire-independent and Fire-sensitive,**  
152 **Fire-dependent on the left (HARDESTY et al. 2005) and Natural vegetation (Forests,**  
153 **Grasslands and Savannas) and Non-natural vegetation (Pasture, Cropland and Forest**  
154 **Plantations) in 2019 in Brazil on the right. (B) NAT's mean burned area percentage per**



155 **pixel is on the left and NON is on the right. The maps show the mean for August,**  
156 **September and October from 2002 to 2019.**

157

158 The target and independent variables were extracted for August, September, and October, from  
159 2002 to 2019, representing the general peak of the fire season in Brazil. This time frame is the  
160 most extended overlapping period between the datasets which we further divided into a training  
161 phase from 2002 to 2009 and a validation phase from 2010 to 2019. The independent variables  
162 were divided into five groups (climate, anthropogenic and natural ignition, fuel, LULC and  
163 forest metrics) and are described in Table 1. We acquired climate variables from the first  
164 component of the third simulation round of the Inter-Sectoral Impact Model Intercomparison  
165 Project (ISIMIP3a, <https://www.isimip.org/>). ISIMIP is a collaborative effort to compare and  
166 evaluate the outputs of various climate and impact models (FRIELER et al., 2023). This data  
167 represents the historical simulations using climate-forcings from GSWP3-W5E5, available  
168 from 1901 to 2019 at a 0.5° spatial resolution.

169 We obtained soil, vegetation carbon and soil moisture from the Joint UK Land Environment  
170 Simulator Earth System impacts model at version 5.5 (JULES-ES; MATHISON et al., 2023)  
171 and driven by ISIMIP3a GSWP3-W5E5 as per Frieler et al. (2023), which is freely available  
172 at <https://www.isimip.org/impactmodels/details/292/>. JULES-ES has previously been used as  
173 input for Bayesian-based fire models (e.g. UNEP et al., 2022). JULES dynamically models  
174 vegetation, carbon fluxes and stores in response to meteorology, hydrology, nitrogen  
175 availability, and land use change. JULES-ES has been extensively evaluated against snapshots  
176 and site-based measurements of vegetation cover and carbon (MATHISON et al., 2023;  
177 WILTSHIRE et al. 2021; BURTON et al., 2019; BURTON et al. 2022). As per UNEP et al.  
178 (2022), vegetation responses to JULES-ES's internal fire model were turned off so as not to  
179 double-count the effects of burning. The maps, therefore, represent environmental carbon  
180 potential and are applicable to FLAME as the model only assumes that variable ranges are  
181 correctly ranked – i.e. areas of low/high carbon content correspond with real-world areas of  
182 low/high carbon and not that the absolute magnitude is correct.

183 Regarding ignition variables, Population Density data was also obtained from the ISIMIP3a  
184 protocol and based on data from the History Database of the Global Environment (HYDE) v3.3  
185 (VOLKHOLZ et al., 2022). Lightning was prescribed as a monthly climatology from LIS/OTD  
186 data (CECIL, 2006). The LIS/OTD Climatology datasets comprise gridded climatologies that



187 document the lightning flash rates detected by the Optical Transient Detector (OTD) and the  
188 Lightning Imaging Sensor (LIS) aboard the Tropical Rainfall Measuring Mission (TRMM).  
189 We collected road density data from the Global Roads Inventory Project (GRIP) (MEIJER et  
190 al. 2018), using total density in  $\text{m}/\text{km}^2$ , which we regrided to the 0.5-degree grid used by the  
191 rest of the data using linear interpolation in the Iris Python package (MET OFFICE, 2023).

192

193 We used the collection 7 LULC data from the MapBiomas project, which produces annual  
194 LULC mapping for the Brazilian territory. They were regrided from 30 m to 0.5° to match  
195 the coarser resolution and interpolated from an annual to a monthly time step.

196

197 The forest metrics variables were calculated into the 0.5° grid based on the forest data from the  
198 Mapbiomas at 30m resolution using the package ‘landscapemetrics’ available in R  
199 (HESSELBARTH et al., 2023). The metrics were number of patches (NP) and edge density  
200 (ED):

201

$$202 \quad NP = n_i \quad (1)$$

203 where  $n_i$  is the number of patches belonging to class  $i$ . NP is an ‘Aggregation metric’ and  
204 describes the fragmentation of a class, in this case, forest formations.

205

$$206 \quad ED = \frac{\sum e_i}{A} \quad (2)$$

207 where  $e_i$  is the total edge length in meters, and A is the total landscape area in square meters.  
208 It quantifies edge density by summing up all edges within class  $i$  in relation to the overall  
209 landscape area. This metric provides insights into the landscape's configuration. We  
210 incorporated these metrics to integrate fragmentation variables - studies suggest that these are  
211 linked to fire occurrence in Amazonia and Cerrado (SILVA JUNIOR et al., 2022; ROSAN et  
212 al., 2022) but remain unexplored in the other biomes.

213

214



Group	Variable	Abbreviation	Source
CLIMATE	Maximum Temperature (°C)	tmax	ISIMIP3a FRIELER et al. (2023)
	Precipitation (m/sec)	ppt	
	Vapor pressure deficit (Pa)	vpd	
	Relative Humidity (fraction)	rh	
	Consecutive number of dry days (days)	dry_days	
	Soil Moisture (fraction)	soilM	JULES-ES
IGNITION	Lightning (flashes/km/day)	lightn	ISIMIP3a FRIELER et al. (2023)
	Population density (people/1000 km <sup>2</sup> )	pop	
	Road density (m/m <sup>2</sup> )	road	GRIP global (MEIJER et al., 2018)
FUEL	Vegetation carbon (kg/m <sup>2</sup> )	cveg	JULES-ES
	Soil carbon (kg/m <sup>2</sup> )	csoil	JULES-ES
LULC	Forest (%)	forest	MAPBIOMAS, 2022
	Grassland (%)	grass	
	Savanna (%)	sav	
	Cropland (%)	crop	





	Pasture (%)	pas	
FOREST METRICS	Number of patches	np	Calculated from MAPBIOMAS, 2022
	Edge density (m/m <sup>2</sup> )	ed	

215

Table 1. Initial list of explanatory variables.

216 **2.2 Variables selection**

217

218 In constructing our predictive model, we considered the interrelationships among different  
 219 variables to ensure a robust and coherent analysis. The selection of variables was guided by  
 220 their correlation, aiming for a set of features that provided information without redundancy.  
 221 For this, we calculated the Spearman correlation coefficient (SPEARMAN, 1961) presented in  
 222 Fig. 4.2. We chose Spearman rank over other correlation metrics as our model has a non-linear  
 223 relationship between drivers and fires (Section 2.3), making it a better assessment than  
 224 parametric comparisons. We identified variables that exhibited strong relationships by  
 225 examining the correlation matrix, which we removed from the final model. We used a threshold  
 226 higher than 0.6 from Spearman’s coefficient for this. The selection was also based on previous  
 227 knowledge about the variables relationship with burned area. For example, we did not include  
 228 lightning even though it presented low correlation with other variables. Fires caused by  
 229 lightning are uncommon and usually occur during the wet season (MENEZES et al., 2022)  
 230 which is out of scope of our analysis.

231

232



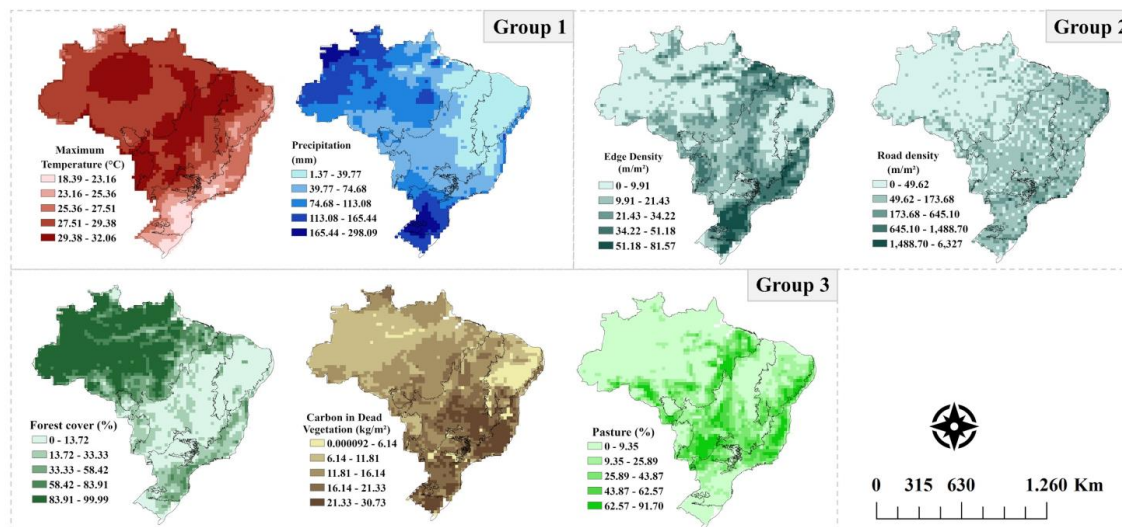
233

234 **Figure 2: Spearman correlation of the explanatory variables. Crossed values indicate no**  
 235 **correlation, values near 1 [magenta] indicate a strong positive correlation and near -1**  
 236 **[cyan] a strong negative correlation.**

237 We adopted a more streamlined approach by opting for a shorter list of variables and by  
 238 grouping them in the variables analysis to capture their compound effect. Initially, we selected  
 239 7 variables as input for the final model (Fig. 3) from the 18 initial variables. These variables  
 240 were chosen based on their correlation, ensuring that at least one variable from each group was  
 241 selected (Climate, Fuel, LULC, Ignition and Forest Metrics). Next, we divided the variables  
 242 into three groups. Group 1 is composed of climate variables Maximum Temperature and  
 243 Precipitation; Group 2 includes the variables Edge Density and Road Density which are related



244 with landscape fragmentation; and Group 3 encompasses Forest cover, Pasture cover and  
 245 Carbon in dead vegetation which are associated with fuel availability.  
 246



248 **Figure 3: Mean of the selected explanatory variables for August, September and October**  
 249 **from 2002 to 2019.**

250

### 251 2.3 Relationship curves

252

253 The constraints or priors of the model were added as parameters of different functions, which  
 254 we refer to as relationship curves. We included the linear and power functions (Fig. 4)  
 255 according to known relationships between fires and environmental variables. This means that  
 256 some environmental variables, when presenting higher values, are likely to increase fires. In  
 257 comparison, others have an inverse relationship where lower values of the variable coincide  
 258 with an increase in burned area. We expect our selected variables to have the following  
 259 relationship with fires:

- 260 1. Maximum Temperature, Carbon in dead vegetation and Pasture are expected to increase  
 261 burning with the increase of the variable (CANO-CRESPO et al., 2015; DOS SANTOS  
 262 et al., 2021; LIBONATI et al., 2022);
- 263 2. Precipitation and Forest, which we expect to increase burning with the decrease of the  
 264 variable (ARAGÃO et al., 2008; BARBOSA et al., 2022);
- 265 3. Edge Density and Roads are expected to have more uncertain response across the  
 266 biomes. High density of edges can lead to more fires into forest ecosystems

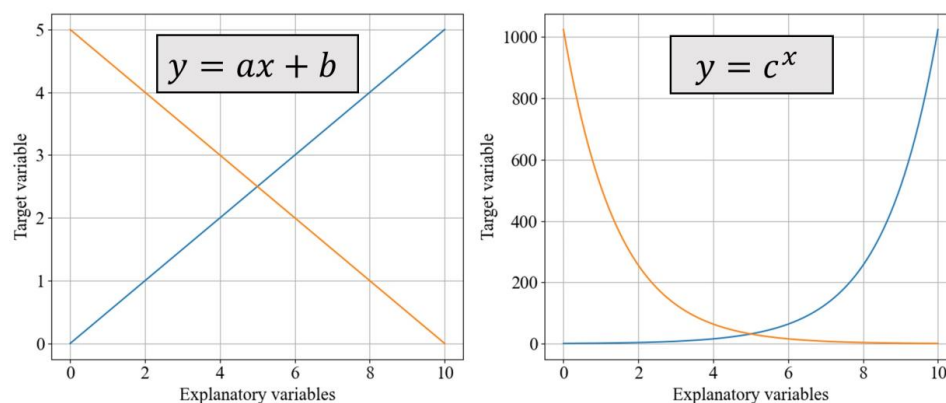


267 (ARMENTERAS et al., 2013; SILVA-JUNIOR et al., 2022) but fragmentation can also  
268 reduce fires by impeding fire spread (DRISCOLL et al., 2021). Regarding Road  
269 Density, while more fires are expected surrounding roads (ARMENTERAS et al.,  
270 2017), less fires are expected with increased density due to urbanization.

271

272 The model then estimates the contribution of each curve to the final model. Even though it is  
273 possible to include more relationship curves, we decided to keep it at a minimum to avoid  
274 making too many assumptions and unstable results due to computational efficiency.

275



276

277 **Figure 4: Graphical representation of the relationship functions implemented in the**  
278 **model. The one on the left is a linear function and on the right is a power function.**

279

280

## 281 2.4 Model optimization

282

283 The model was optimized for each Brazilian biome separately using the MCD64A1 product  
284 from 2002 to 2009. This process used the PyMC5 Python package (ABRIL-PLA et al., 2023),  
285 employing 5 chains each over 1000 iterations using the No-U-Turns Hamilton Monte Carlo  
286 sampler (HOFFMAN and GELMAN 2014) while utilizing 20% of the data or a minimum of  
287 6000 grid cells. While the runs were conducted individually for each Biome, the results were  
288 aggregated to facilitate visualization. The code used to develop this model is available on  
289 GitHub repository (<https://github.com/malu-barbosa/FLAME>).

290

291 In Bayesian inference, we update our beliefs or knowledge about a system or event by  
292 incorporating new evidence or data (LAPLACE, 1820; GELMAN et al., 2013). It allows us to



293 quantify and update our uncertainty using probability distributions. By maximizing entropy,  
294 we aim to achieve the most unbiased, information-rich distribution that satisfies this prior  
295 knowledge. In this sense, the likelihood (or posterior probability) of the values of the set of  
296 parameters,  $\beta$ , given a series of observations  $Obs_i$  and explanatory variables ( $X_{iv}$ , from section  
297 2.2) is proportional ( $\propto$ ) to the prior probability distribution of  $P(\beta)$  multiplied by the  
298 probability of the observations given the parameters tested.

299

$$300 \quad P(\beta | \{Obs_i\}, \{X_{iv}\}) \propto P(\beta) \times \prod_i P(Obs_i | \{X_{iv}\}, \beta) \quad (3)$$

301

302 Where  $\{Obs_i\}$  is a set of our target observations, and  $i$  is the individual data point and  $\{X_{iv}\}$  is  
303 the set of explanatory variables,  $v$ , for data point  $i$ . The  $\pi$  notation ( $\Pi$ ) indicates repeated  
304 multiplication. Maximum Entropy in species distribution modeling assumes that individual  
305 observations ( $Obs_i$ ) are either 1 when there is a fire or 0 when there is not, and that:

$$306 \quad P(1 | \{X_v\}, \beta) = f(\{X_v\}, \beta) \text{ and } P(0 | \{X_v\}, \beta) = 1 - f(\{X_v\}, \beta) \quad (4)$$

307 Where  $P(1 | X, \beta)$  is the probability of a fire to occur,  $P(0 | X, \beta)$  is the probability of no fire.

308 The term  $f(X, \beta)$  is defined below:

$$309 \quad f(\{X_v\}, \beta) = 1 / (1 + e)^{-y(\{X_v\}, \beta)} \quad (5)$$

310 where  $y(\{X_v\}, \beta) = \text{linear function} + \text{power function}$  (section 2.3):

$$311 \quad y(\{X_v\}, \beta) = \beta_0 + \sum_v (b_{0,i} \times X_v + b_{1,v} c^{X_v}) \quad (6)$$

312

313 This works for single land points, where a location burns or does not burn. We extend this  
314 concept to derive the Maximum Entropy solution for fractional burned area by integrating over  
315 a larger grid cell area. Here we consider that when dividing a gridcell indefinitely, the subcell  
316 sizes approach infinitesimally small values and the data within each subcell starts to behave  
317 like continuous data. We adapted Eq. (3) and (4) to work with continuous data:

$$318 \quad P(\beta | \{Obs_i\}, \{X_{iv}\}) \propto P(\beta) \times \prod_i^n \prod_j^s P(Obs_{ij} | \{X_{iv}\}, \beta)^{1/s} \quad (7)$$

319 Where  $n$  is the observations sample size,  $j$  is the individual subgrid, and  $s$  is the subgrid sample  
320 size. If, for a given  $Obs_i$ ,  $m$  of the  $s$  subgrid cells burn, then we can adapt Eq. (4) to get:



$$\begin{aligned} 321 \quad P(m/s | \{X_{iv}\}, \beta) &= \prod_j^s P(I | \{X_{iv}\}, \beta)^m \times P(0 | \beta)^{s-m} \\ 322 \quad &= f(\{X_{iv}\}, \beta)^m \times (1 - f(\{X_{iv}\}, \beta))^{m-s} \end{aligned} \quad (8)$$

323 and therefore:

$$324 \quad P(\beta | \{m_i/s_i\}, \{X_{iv}\}) \propto P(\beta) \times \prod_i^n f(\{X_{iv}\}, \beta)^{m/s} \times (1 - f(\{X_{iv}\}, \beta))^{(m-s)/s} \quad (9)$$

325 When  $s \rightarrow \infty$ ,  $m/s$  becomes burned area fraction (BF). Then:

$$326 \quad P(\beta | \{BF_i\}, \{X_{iv}\}) \propto P(\beta) \times \prod_i^n f(\{X_{iv}\}, \beta)^{BF_i} \times (1 - f(\{X_{iv}\}, \beta))^{1-BF_i} \quad (10)$$

327 This solution assumes that burning conditions at a specific location solely explain the  
328 likelihood of burning. In reality, fires spread and, particularly at higher burned areas, they may  
329 overlap. We, therefore, modify  $Obs_i$  so that it represents what the burned fraction of a gridcell  
330 would look like if it was one large fire with no overlapping burning:

$$331 \quad Obs_i = Obs_{i,0} \times (1 + Q) / (Obs_{i,0} \times Q + 1) \quad (11)$$

332 Where  $Obs_{i,0}$  is the true observation, and  $Q$  is a modifier parameter to remove the effects of  
333 fire overlap.

334 Lastly, to account for variations in land cover to assign between natural and non-natural  
335 vegetation, which can be very small in some cells, we introduced a weighting factor  $w$  when  
336 assessing fire categories. This weighting factor considers the individual area of each grid cell,  
337 ensuring that cells with smaller vegetation cover contribute proportionally to the analysis, as  
338 in Eq. 12 below:

$$339 \quad P(\beta | \{BF\}, \{X_{iv}\}) \propto P(\beta) \times \prod_i^n f(\{X_{iv}\}, \beta)^{BF_i \times w} \times (1 - f(\{X_{iv}\}, \beta))^{(1-BF) \times w} \quad (12)$$

340 We use weak, uninformed prior distributions for our Eq. (6) parameters.  $\beta_0$ ,  $b_{0,i}$  and  $b_{1,i}$  priors  
341 were set as a normal distribution with a mean of 0 and a standard deviation of 100, and  $c$  a  
342 lognormal with a  $\mu$  of 0 and a  $\sigma$  of 1.

343

344

## 345 **2.5 Model evaluation**

346

347 The model's main goal is to accurately quantify uncertainties, which we tested by analyzing  
348 where the observations fell in the model's posterior probability distribution (Eq. 10). If more



349 than 20% of the observations fall outside the 10th-90th percentile range, the uncertainty range  
350 is too narrow. Conversely, if observations cluster around 50%, the uncertainty range is too  
351 wide. We aim to minimize uncertainty constraints without compromising accuracy. When  
352 evaluating the model against 2010-2019 observations, we also investigated how likely the  
353 observations are given the optimized model ( $P(\text{Observed}|\text{Simulated})$ ), as per Kelley et al.  
354 (2021). Using a different time period from the optimization, we ensure an independent model  
355 evaluation. If the out-of-sample observations are more likely given the model, then the model  
356 performs well. We use a likelihood of 50% to indicate adequate performance.

357

358 We calculate the probability of an observation given our model by integrating the observation's  
359 likelihood across parameter space, weighted by the parameter likelihood given our training in  
360 section 2.4:

$$361 \quad P(Y | (X, \beta | \{BF_0\}, \{X_0\})) = \int_{\beta} P(\beta | \{BF_i\}) \times P(Y | \beta) d\beta \quad (13)$$

362

363 which, combined with Eq. (10), gives us:

364

$$365 \quad P(Y | (X, \beta | \{BF_0\}, \{X_0\})) = \int_{\beta} P(\beta | \{BF_i\}) \times f(X, \beta)^Y \times (1 - f(X, \beta))^{1-Y} \quad (14)$$

366

367 Where  $Y$  is an observation and  $X$  corresponds to the model inputs at the time and location of  
368  $Y$ . We approximate this by sampling 200 parameter ensemble members from each of our five  
369 chains, providing us with 1000 ensemble members. The frequency of these 1000 in parameter  
370 gives us " $P(\beta | \{BF_i\})$ " in Eq. (14). We then drive the model with each parameter combination  
371 to give us  $f(X, \beta)$ . We used the iris package (MET OFFICE, 2023) with Python version 3  
372 (Python Software Foundation, <https://www.python.org/>) for sampling.

373

374 We also determined the percentile of our observations within the model's posterior probability  
375 distribution. In an unbiased model, we expect the observation position to be essentially random,  
376 with the mean over many samples tending towards the middle of the distribution (i.e., a  
377 percentile of 50%). We mapped out the mean position of the observations for the 30 time steps  
378 (3 months, August, September, October, for 10 years) tested (Fig. 6). The p-value in Fig. 7  
379 uses the student t-test to ascertain if the mean of the posterior position of the monthly  
380 observations for a given gridcell (mean bias) is significantly different 50% (i.e., the model is  
381 biased). A mean bias near 0 indicates that observations are consistently smaller than the





382 simulations, and near 1 indicates that the observations are greater than the simulations. Low p-  
383 numbers indicate where the model is biased towards a probability distribution, which tends to  
384 suggest too low or high burning.

385

## 386 **2.6 Variables analysis**

387

388 We assessed the behavior of the variables against the burned area simulations by generating  
389 response maps for our variable groups in a similar way to Kelley et al. (2019). In the potential  
390 maps, we set each variable in the group to their median and kept the others at their original  
391 values. The median, representing the middle value in a dataset, was chosen because it is less  
392 affected by extreme values compared to the mean. The maps were subtracted from the original  
393 simulations (control - potential response) to quantify the influence of the target group on the  
394 model's response. This approach enables the assessment of burned area response when the  
395 variable deviates from the median and assumes its original values. The agreement maps for the  
396 potential response are then the percentage of the modeled distribution that shows an increase  
397 in burning in each Biome. To compute the sensitivity response, we took the difference between  
398 a simulation where we subtracted 0.05 and added 0.05 fraction of the training range of the  
399 variable of interest. The goal was to understand how burned area responds to marginal  
400 variations in the variables.

401

## 402 **3 RESULTS**

403

404 We present the results in two sections. The first section focuses on the model's performance in  
405 simulating the observations, while the second section delves into the simulation's response to  
406 the predictor variables.

407

### 408 **3.1 Model simulations and performance**

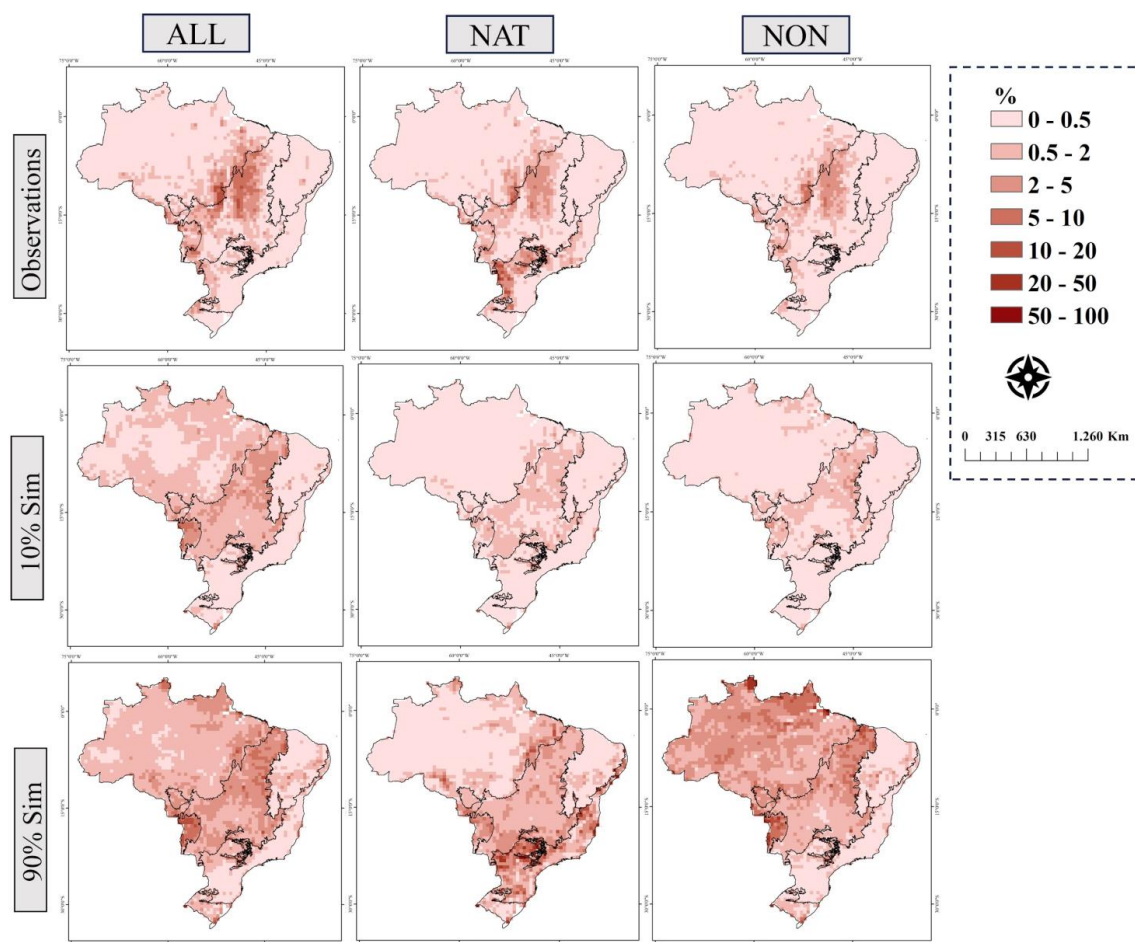
409

410 We performed simulations of burned area across each Brazilian biome and fire category, and  
411 the resulting maps are shown in Fig. 5. The three simulation runs (ALL, NAT, and NON)  
412 successfully captured uncertainties in all Biomes, with most observations falling within the  
413 10th to 90th percentiles of the model. However, the model exhibits variations in uncertainties  
414 based on the simulation category. For instance, in Amazonia, a biome characterized by a vast  
415 expanse of natural vegetation, uncertainties were smaller in NAT simulations, contrasting with  
416 larger uncertainties observed in NON-simulations, especially in areas where observed burned





417 areas are small or zero (Fig. 5). Similarly, the Pantanal displayed lower uncertainties in NAT  
418 simulations, with values reaching up to 10%, while NON simulations registered uncertainties  
419 up to 20% of burned area. The Atlantic Forest, a biome distinguished by non-natural vegetation,  
420 exhibited smaller uncertainties in NON simulations. These findings indicate that the  
421 segregation of fire categories (ALL/NAT/NON) substantially impacts the model's response.  
422 Conversely, the model struggles to accurately capture large burned areas (> 10%) in central  
423 regions of Brazil across all three simulations, mostly where the Cerrado biome is located.



425 **Figure 5: Maps of modeled and observed % burned area. First row: observed burned area,**  
426 **July-September 2002-2009 annual average for ALL (left), NAT (middle) and NON (right).**  
427 **Second and third row: as top row but simulated by the model 10th and 90th percentiles,**  
428 **respectively.**

429



430 In Bayesian inference, the likelihood expresses the probability of observing a particular event  
 431 given the model's parameters. Our results imply a strong agreement between the parameters of  
 432 the model and the observations (Table 2), even during the months when the observations were  
 433 less likely. The mean likelihood during these months was above 90% across all Biomes in all  
 434 simulations, except for the Pantanal, where the likelihood was lower (78% for ALL and 87%  
 435 for NON) but still satisfactory. The percentiles indicated that in the Pantanal, the likelihood of  
 436 the observations for ALL varied between 59% to 91%. In contrast, other Biomes presented a  
 437 minimum likelihood of 80%. During months of best performance, most biomes aligned with  
 438 the observations, achieving its maximum likelihood (100%) on average. The Pantanal,  
 439 however, presented the lowest values, with 97% for both ALL and NON simulations.

440

441 **Table 2.** Likelihood (%) per biome of the observations given the model parameters over all  
 442 cells and timesteps. 10% (left) indicates months/cells with worst performance, while 90%  
 443 (right) indicates best performance.

	Worst performance			Best performance		
Likelihood - All fires						
Biome	Mean	10th percentile	90th percentile	Mean	10th Percentile	90th Percentile
Amazon	95	89	99	99	98	100
Caatinga	99	98	100	100	100	100
Cerrado	90	80	97	99	98	100
Atlantic Forest	99	97	100	100	100	100
Pampa	96	92	100	99	98	100
Pantanal	78	59	91	97	93	100
Natural						
Amazon	98	95	100	100	100	100
Caatinga	99	99	100	100	100	100
Cerrado	95	91	99	100	99	100
Atlantic Forest	99	98	100	100	100	100
Pampa	97	95	100	99	98	100
Pantanal	92	86	98	100	99	100
Non - natural						
Amazon	95	91	99	99	98	100
Caatinga	99	99	100	100	100	100
Cerrado	94	88	99	99	98	100
Atlantic Forest	99	98	100	100	100	100
Pampa	97	94	100	99	98	100
Pantanal	87	78	96	97	93	100

444

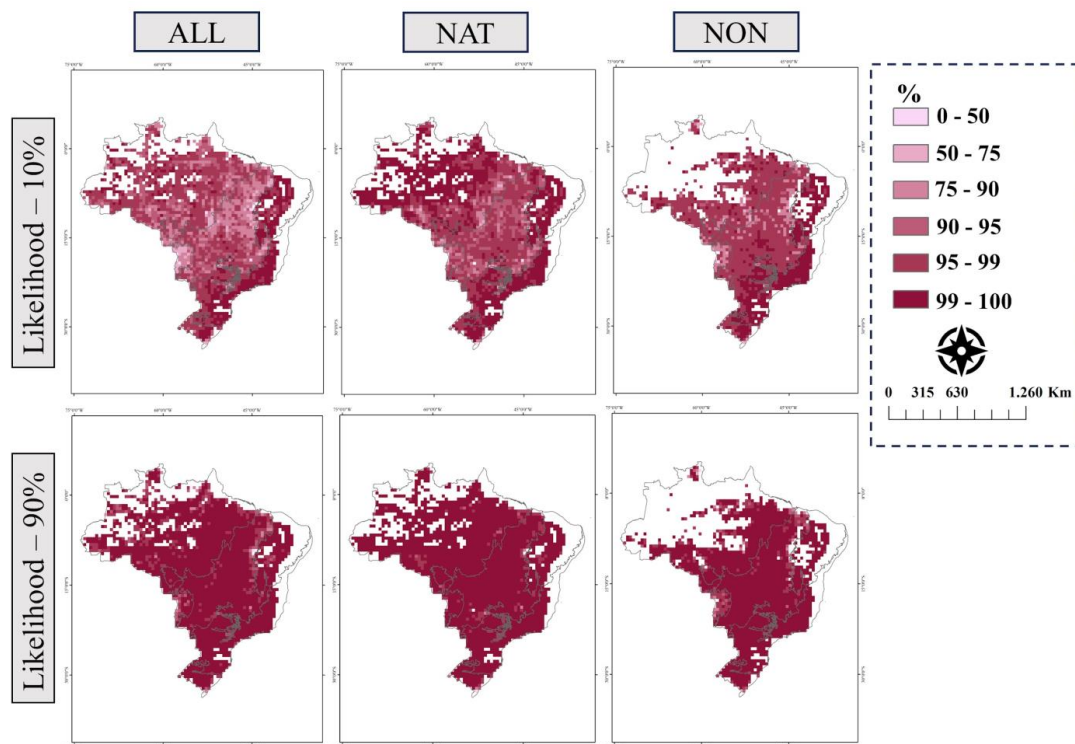
445

446

447 Figure 6 presents the likelihood per pixel. Areas without values indicate zones where burned  
 448 area is zero, making the likelihood calculations inapplicable. The spatial likelihood analysis



449 provides additional insights into the model's robustness across different biomes and fire  
450 categories. The results underscore the model's effective performance across the biomes.  
451 Notably, the likelihood remained very high for the Atlantic Forest, Caatinga, and Pampa  
452 biomes even in the months and locations where observations were less likely. A high likelihood  
453 is also observed for NAT in Amazonia, except for the south and east, which contain most of  
454 the non-natural vegetation. Lower performance is evident in the simulations for both ALL and  
455 NON in this Biome, indicating that stratifying fire categories by vegetation type could be a good  
456 strategy to enhance model performance in Amazonia, or isolating fire categories where the  
457 model has higher predictive ability. Similarly, the Pantanal showed the best performance for  
458 NAT, but lower performance for ALL and NAT across the majority of the Biome. In contrast,  
459 Cerrado performed better than most biomes for NON during the months of worst performance.  
460



462

463 **Figure 6: Spatial likelihood of the observations given the model parameters considering the**  
464 **months with worst performance (top row) and the months with best performance (bottom**  
465 **row). A satisfactory performance of the model is considered with values above 0.5.**

466



467  
468 Despite the high likelihood associated with the observations, the model simulations exhibit a  
469 certain degree of bias across the three categories. A mean bias near 0.5 indicates no bias, as the  
470 observations fall in the middle of the model's distribution. Amazonia and Cerrado showed mean  
471 biases of 0.28 and 0.29 for ALL respectively, indicating an overestimation by the simulations  
472 at lower burned areas. The Atlantic Forest presented a mean bias of 0.51, suggesting that,  
473 overall, the model is unbiased although some pixels may still be biased. Similarly, Pampa  
474 (0.42) and Caatinga (0.61) showed values near 0.5, indicating a lower degree of bias. In  
475 contrast, a mean bias of 0.17 in the Pantanal suggests an overestimation of burned area by the  
476 model, especially at lower levels. However, the model can distinguish between lower and high  
477 burned areas in Pantanal (Fig. 5), indicating its ability to identify periods and locations of more  
478 extreme burning, even if it does not exactly capture the correct magnitude.

479  
480 Generally, higher uncertainties are observed for NAT and NON simulations, but a notable  
481 improvement in bias is evident when compared to the ALL simulations. In the NAT  
482 simulations, the model achieved its most favorable outcomes in Pampa (0.53) and Amazonia  
483 (0.40), with the Pantanal also showing a noticeable improvement (0.34). The biases of 0.74 in  
484 Caatinga and 0.72 in the Atlantic Forest indicate a trend toward underestimation in this fire  
485 category. In Cerrado, a bias value of 0.33 was observed for NAT, aligning with the pattern seen  
486 in the ALL simulations and suggesting a consistent overestimation, particularly for lower  
487 burned areas.

488  
489 In the NON simulations, Amazonia exhibited a bias of 0.38 but overestimated lower burned  
490 areas. Cerrado and Pantanal showed similar patterns to those in the NAT simulations, with  
491 respective mean biases of 0.36 and 0.31. The model tended to underestimate burned areas in  
492 the Caatinga (0.81), particularly at higher burned areas. While Atlantic Forest (0.58) and Pampa  
493 (0.59) showcased the most unbiased simulations for the NAT fire category, slight  
494 underestimation of burned areas were noted in some instances (Fig. 7).

495  
496 The spatial distribution of the mean bias, as depicted in Fig. 7, exhibits considerable variation.  
497 Pixels without values indicate zero burned area in the observations, where, by definition, the  
498 observation will always fall at the 0th percentile of the model posterior distribution.  
499 Consequently, the bias metric does not provide meaningful information for these pixels. The  
500 p-values reveal that in numerous areas, the bias is not statistically different from 0.5 (p-value

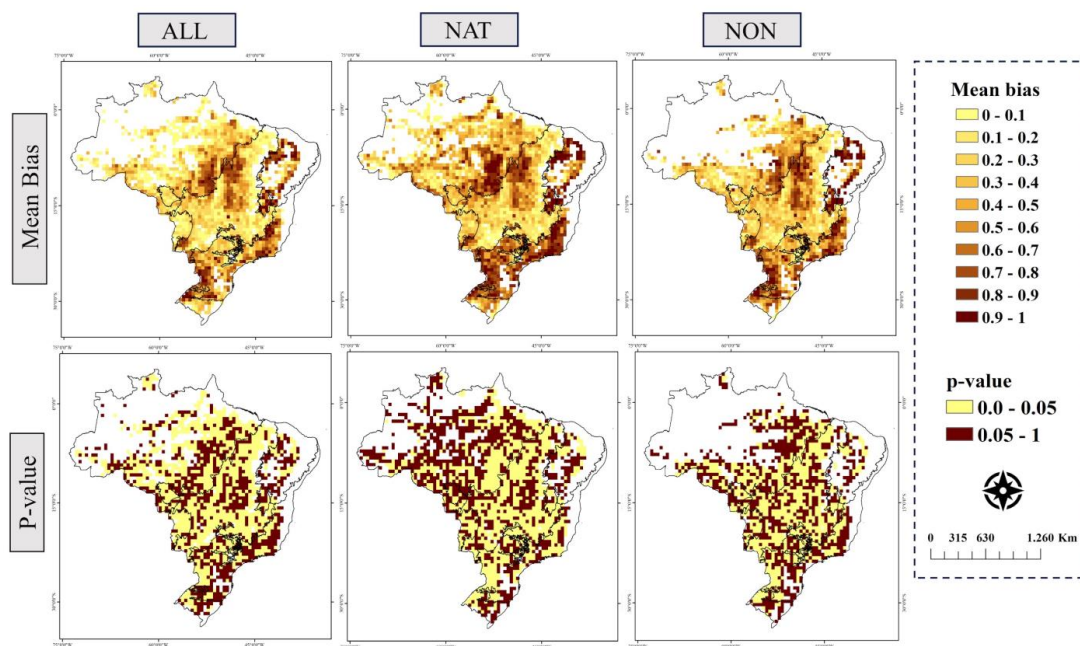


501 > 0.05; indicated by brown color), suggesting unbiased simulations in these regions.  
502 Specifically, lower fires in Amazonia tend to occur in areas of natural vegetation, where NAT  
503 simulations exhibit a non-significant bias. In these regions, ALL simulations tend to  
504 overestimate burned area. In southeastern Amazonia, fires were underestimated across all three  
505 fire categories, especially for NAT.

506

507 In Caatinga, all three simulations exhibited similar performance, significantly underestimating  
508 fires, particularly in the northern part of the Biome. The Atlantic Forest displayed better results  
509 for both ALL and NON, with a substantial area exhibiting non-significant bias. The fragmented  
510 landscape of this Biome likely limits data availability for NAT, possibly explaining the lower  
511 performance in this fire category. In contrast, Cerrado demonstrated a consistent pattern across  
512 all three fire categories, predominantly overestimating fires, especially in the south and  
513 northeast. While some underestimation occurred in the central biome, it was mostly non-  
514 significant. In Pantanal, the simulation consistently overestimated burned area across all three  
515 categories, with ALL simulations showing significant overestimation throughout the Biome.  
516 Finally, Pampa displayed a non-significant bias across most of the region, except for the  
517 northwest, where the model underestimated burning in all three simulations.

518





520

521 **Figure 7: Top row: Spatial mean bias of the modeled burned area to ALL (left), NAT**  
522 **(middle) and NON (right). Bottom row: Significance of the mean bias considering a 95%**  
523 **confidence level (p-value < 0 .05). Pixels with p-value > 0.05 (brown color) are not**  
524 **significantly different from 0.5 mean bias meaning that they are unbiased.**

525

### 526 **3.2 Response of the modeled burned area to the explanatory variables**

527

528 We assessed the potential and Sensitivity responses of the variables (Fig. 8, 9 and 10). The  
529 potential response offers insights into changes in burned area when variables deviate from the  
530 median, thereby identifying areas where responses tend to drive or suppress burning. In  
531 contrast, the sensitivity response provides information on how marginal changes in variables  
532 affect burned area (KELLEY et al. 2019). Together, these analyses highlight areas susceptible  
533 to more extreme burning (i.e., where the burned area is sensitive to variables that tend to cause  
534 higher potential burning).

535

536 For ALL burned area (Fig. 8), variations of Group 1 (Maximum Temperature and Precipitation)  
537 from the median is very likely to lead to an increase in the burned area in 62.33% of Amazonia  
538 (with a likelihood of over 80%). This means that when these variables assume their actual  
539 values in this Biome, the burned area tends to be higher, with increases up to 1% in the western  
540 edge and 10% in the north, northeastern and southeastern of the biome. Conversely, these  
541 variations contributed to a reduced burned area in 33.57% of Amazonia, predominantly  
542 observed in the western and central areas, suggesting that Maximum Temperature and  
543 Precipitation tend to suppress burned area in these regions. In 4.08% of the biome, the influence  
544 of Group 1 variables on burned areas is not confidently predictable in terms of whether they  
545 will lead to an increase or decrease (with likelihood between 40% and 60%), and the model  
546 showed strong confidence only in the regions where these variables are major drivers and  
547 suppressors of burning. Our results indicate that the entire Amazon is highly sensitive to minor  
548 variations in Group 1 variables for ALL (Fig. 8). Nonetheless, the middle and western regions  
549 tended to be up to three times less sensitive than the rest of the biome.

550

551 In the Atlantic Forest, approximately 63.33% of the biome will likely experience an increase  
552 in burned areas when Temperature and Precipitation assume their real vs median values, mostly  
553 limited to 1% extra burning. This small increase highlights that these drivers do not have a  
554 major influence on driving high levels of total burned area. Reduction of burned area is





555 observed in the western portion, encompassing 31.79% of the biome. Uncertainties linked to  
556 Group 1 variables were found in 4.87% of the Atlantic Forest. Moreover, this biome showed  
557 an overall lower sensitivity to climate.

558

559 In Cerrado, Group 1 is likely to drive burned area up to 6% in 58.30% of the biome, primarily  
560 in the eastern part. Conversely, 37.16% of Cerrado is expected to observe a reduced burned  
561 area by up to 10%, showing quite a range in the influence in mean burned area from the variable  
562 group. The remaining 4.53% of the area remains uncertain. Cerrado exhibited high sensitivity  
563 to changes in Group 1, except for the central region of the biome, which showed comparatively  
564 lower sensitivity. In the Pantanal, the central and northern areas are likely to experience an  
565 increase in burned area by up to 1% due to variations in Group 1, accounting for 51.92% of  
566 their total area. Conversely, the borders of the Pantanal, particularly the south, exhibited a  
567 reduction in burned area (42.30% of the Pantanal). Approximately 5.76% of the Pantanal  
568 landscape remains uncertain regarding the direction of changes. The entire biome presented  
569 considerable sensitivity for small variations in Group 1. Pampa exhibited a high likelihood of  
570 increased burned area in 70.14% of the region, mainly limited to 1%. We found a high  
571 likelihood of reduction in 26.86% of Pampa, located in the northwestern, and in 2.98% of the  
572 biome it is unclear the direction of changes. Pampa's west and southeastern edges showed to  
573 be more sensitive to Group 1. The southern and eastern portions of Caatinga are likely to face  
574 an increase in burned area by up to 4%, affecting 51.23% of the biome, attributable to the  
575 influence of Group 1. Conversely, 47.34% of Caatinga, particularly in the northern and western,  
576 is more likely that the burned area will diminish, while 1.41% is unclear. In general, the biome  
577 showed less sensitivity to Group 1, with slightly higher sensitivities observed in the central and  
578 northeast of the biome.

579

580 For Group 2 variables (Edge Density and Road Density), 47.37% of Amazonia will likely  
581 experience an increase in burned area when these variables deviate from the median. This  
582 increase is predominantly limited to 1%, concentrated in the western, central, and northeast  
583 regions. Conversely, areas with higher edge and road densities show a reduced burned area of  
584 up to 11%, covering 51.82% of Amazonia. This is a 12% range in burned area, substantial for  
585 a fire-sensitive biome. Overall, the biome displays moderate sensitivity to minor variations in  
586 Group 2, with higher sensitivity observed along its borders. The response in the Atlantic Forest  
587 exhibited more uncertainty in the 10th and 90th percentiles. Still, the likelihood indicates that  
588 42.30% of the biome will likely experience increased burned areas of up to 2%, primarily



589 located in the north and eastern edges. Small reductions are found in 54.87% of the biome,  
590 limited to 0.2%. Regions where increases are more likely also demonstrate greater sensitivity  
591 to Group 2, showing the potential for these drivers to have a disproportionate influence on  
592 extreme levels of burning.

593

594 The Cerrado biome exhibited high spatial variability in response to Group 2, with a nearly  
595 equal mix of pixels where an increase (47.28%) and decrease (44.56%) in burned area is more  
596 likely to occur, both limited to 2.5%. The northeast of the biome displayed higher sensitivity  
597 to Group 2. In Pantanal, the central and southern regions are more likely to experience a  
598 decreased burned area, encompassing 53.84% of the biome. However, an increase is found in  
599 42.30% of Pantanal, limited to 8%. The Pantanal demonstrated sensitivity to Group 2,  
600 especially in the north. In Pampa, 47.76% of the region exhibited increased burned areas, while  
601 reductions occur in 47% of it. Increases reached up to 4%, primarily in the western portion.  
602 These regions where an increase is likely also showed higher sensitivities. In Caatinga, a  
603 reduction in burned area is likely to occur in 50.17% of the biome, while an increase is expected  
604 in 38.86% of it. Approximately 10.95% of the biome remains uncertain about the direction of  
605 change. In areas where results do suggest a confidence change, increases are mainly located in  
606 the middle of the biome.

607

608 In the context of Group 3 variables (Forest, Pasture, and Carbon in dead vegetation),  
609 approximately 53% of Amazonia will likely experience larger burned areas, primarily  
610 concentrated in the arc of deforestation (along the southern and eastern edges of the Amazon),  
611 reaching up to 10%. Conversely, reductions are observed in 42% of the biome, with 4.23%  
612 remaining uncertain. While displaying less sensitivity to minor changes than other groups,  
613 certain areas such as the cross borders with Cerrado and north exhibit higher sensitivity within  
614 the biome. In the Atlantic Forest, increased burned areas are observed in 41.53% of the region,  
615 while reductions are noted in 54.87%. Decreases in the biome are primarily observed in the  
616 central southern and eastern areas, with magnitudes reaching up to 0.7%. Overall, the  
617 sensitivity in this biome is lower although the spatial variation shows heightened sensitivity in  
618 the 90th percentile for some pixels across the biome.

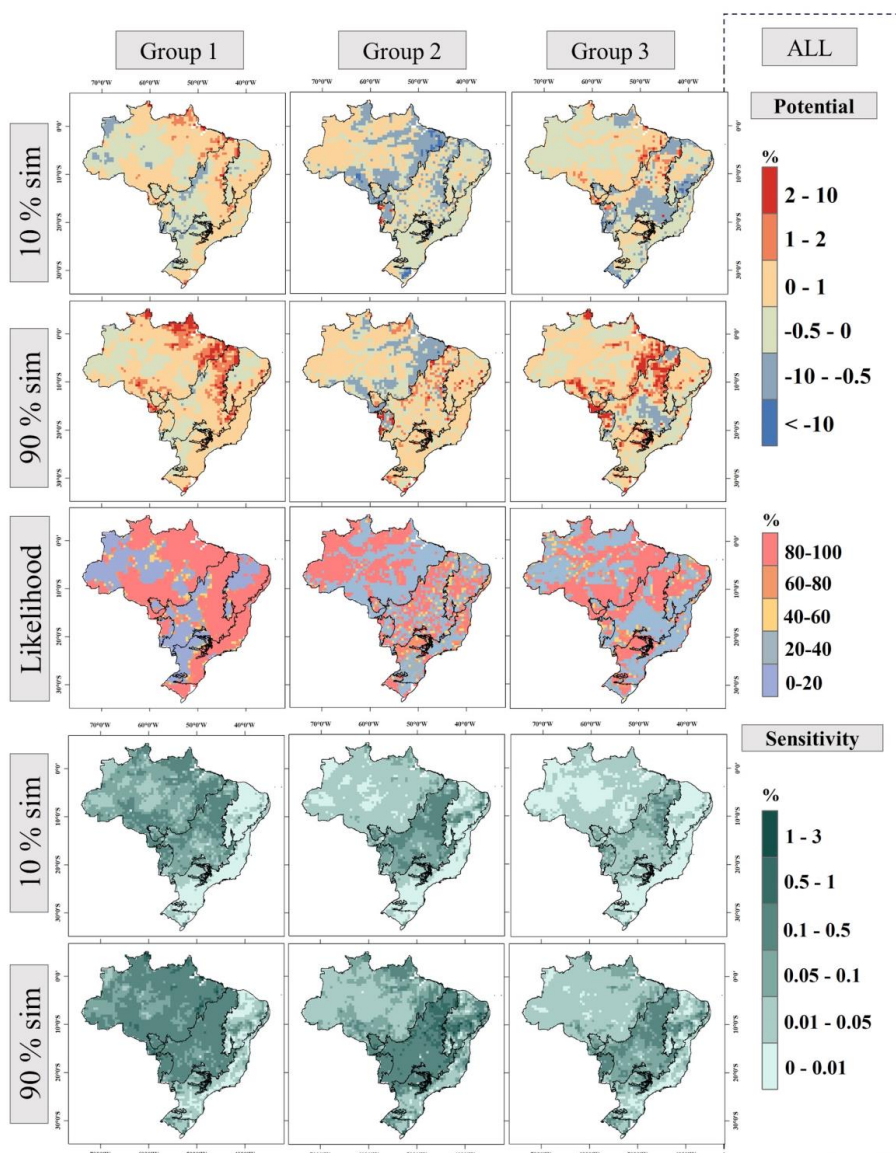
619

620 In the Cerrado biome, burning in the middle south and northeast edges is not likely driven by  
621 Group 3 variables, covering 54.83% of the biome. Conversely, the north, northeast, and part of  
622 the south (39.72% of Cerrado) may experience increased burned areas of up to 10%. Regions





623 with higher likelihood of increase also demonstrate greater sensitivity to small variations in  
624 Group 3. Pantanal shows approximately 30.77% of its area likely to experience up to a 10%  
625 increase in burned areas, mainly in the north and southeastern regions. Conversely, edges and  
626 the southern part are more prone to reductions, encompassing 55.76% of the biome, while 13%  
627 remain uncertain. Pantanal demonstrates high sensitivity overall to Group 3. In Pampas,  
628 52.23% of the region is more likely to see increased burned areas of up to 3.5%, while  
629 reductions are observed in 44.77% of the area. The western part and eastern edges of the biome  
630 show greater sensitivity to minor changes in Group 3. In Caatinga, approximately 53.35% of  
631 the biome is likely to experience reduced burned area while 38.16% is likely to see up to 3%  
632 increases. The central and northeast regions, where increases are expected, also exhibit higher  
633 sensitivity to minor shifts in Group 3.  
634



635  
636 **Figure 8: Response maps to ALL displaying the potential 10h percentile (first row), 90th**  
637 **percentile (second row), likelihood (third row) and sensitivity responses 10th percentile**  
638 **(fourth row) and 90th percentile (fifth rows). Each column presents the results for one**  
639 **group of variables.**  
640

641 Similar spatial patterns to ALL were observed for NAT when considering Group 1 across all  
642 biomes (Fig. 9). In the Amazon, Group 1 will likely increase burned area in 63.79% of the  
643 biome. Reductions are found in 29.92%, while 6.27% display an unclear response. This



644 indicates a 2% increase in areas with uncertain responses, particularly in the southeastern  
645 region of the Amazon. Sensitivity analysis reveals that the borders of the Amazon are more  
646 sensitive to Group 1, whereas areas with forest cover < 83% (Fig. 3) exhibit lower sensitivity.  
647 In the Atlantic Forest, Group 1 is likely to drive burned area changes in 67.95% of the biome.  
648 Conversely, 19.23% is likely unaffected by Group 1, with 12.82% remaining unclear,  
649 representing an 8% increase compared to ALL. The Sensitivity to Group 1 was similar to ALL,  
650 generally lower for this biome.

651

652 In Cerrado, Group 1 contributes to increased burned area in 61.78% of the biome. However, in  
653 32.78% of the area, Group 1 is likely not a driving factor for the burned area, and in 4.53%,  
654 the response is unclear. The biome also exhibits sensitivity to minor variations in Group 1 for  
655 NAT, albeit slightly lower in some areas (Fig. 9) than ALL. In Pantanal, 80.76% of its area  
656 likely has Group 1 as drivers of burned area in NAT, representing an increase of almost 30%  
657 compared to ALL. Areas not influenced by this group decreased by 25% compared to ALL  
658 (15.38% of Pantanal), while 3.84% remains unclear. The sensitivity analysis closely resembled  
659 ALL, with the entire biome significantly responding to variations in Group 1. In Pampas, it is  
660 likely that variations from the median lead to increased burning in 70.14% of the biome.  
661 Sensitivity is similar to ALL, primarily in the west but generally lower. Caatinga follows a  
662 similar pattern to ALL, with Group 1 influencing burning in 48.76% of the biome. Uncertainty  
663 increased to 4.94% of the biome, and sensitivity is similar, affecting mainly the middle and  
664 northeast regions.

665

666 For Group 2, Amazon presented a more uncertain response between the 10th and 90th  
667 percentiles. However, the likelihood showed a marked pattern very similar to ALL where  
668 47.37% of the biome has Group 2 as a driver of burning. Similar to Group 1, the sensitivity  
669 was lower in highly forested areas. For NAT, the Atlantic Forest showed large areas with an  
670 unclear response (Fig. 9), covering 41.79% of the biome. The areas where burning is likely to  
671 be driven by Group 2 encompasses 26.41%, a reduction of 15% when compared to ALL. The  
672 sensitivity was similar to ALL, with slightly higher values in some pixels. The Cerrado showed  
673 variation within the biome, with 45.61% of its area identified as potentially driven by Group 2  
674 in NAT. While the sensitivity was lower than in ALL, it remained significant within Cerrado.  
675 Pantanal exhibited Group 2 as a driver of burning in 46.15% of the biome, displaying a spatial  
676 pattern for the likelihood very similar to ALL. However, sensitivity was lower in the middle  
677 of Pantanal compared to the North and edges. Similarly, Pampa presented a response similar



678 for both potential and sensitivity as in ALL, with 47.76% of areas likely to experience increased  
679 burning driven by Group 2. In Caatinga, areas likely to experience increased burning accounted  
680 for 37.45% of the biome, and the regions with unclear responses were 6.72% higher than in  
681 ALL (17.67%). Sensitivity showed the same pattern as in ALL.

682

683 Amazonia showed a 4% increase in areas with unclear responses for Group 3 to 8.10%  
684 compared to ALL. Regions susceptible to burning due to this group totaled 54.74% of the  
685 biome. Densely forested areas also exhibited lower sensitivity to minor shifts in Group 3. In  
686 Atlantic Forest, Group 3 is likely to be a driver of burned area in 41.02% of the biome, very  
687 similar to ALL (41.53%). Similarly, the sensitivity followed the spatial pattern of ALL with an  
688 overall lower sensitivity presenting slightly higher in some pixels. Areas prone to burning in  
689 the Cerrado due to Group 3 reduced by 10.84%, totaling 43.95% compared to ALL. The  
690 reduction was concentrated in the northeast, while in the southwest there was an increase in  
691 the likelihood of burning due to Group 3. The sensitivity reduced in the northeast, varying  
692 across the biome. Within the Pantanal, regions susceptible to burning due to Group 3 comprised  
693 32.69% of the area. Regions with an unclear response increased by 4.30%, encompassing  
694 17.30% of the region and concentrated in the eastern edges.

695

696 In Pampas, 44.77% of the biome is likely to burn due to Group 3, while 17.30% of the biomes  
697 showed an unclear response. The sensitivity pattern for NAT followed ALL, concentrated in  
698 the western and eastern edges. The Caatinga accounted for 35.68% of areas prone to burning,  
699 with higher sensitivities observed in the middle and eastern regions of the biome.

700

701

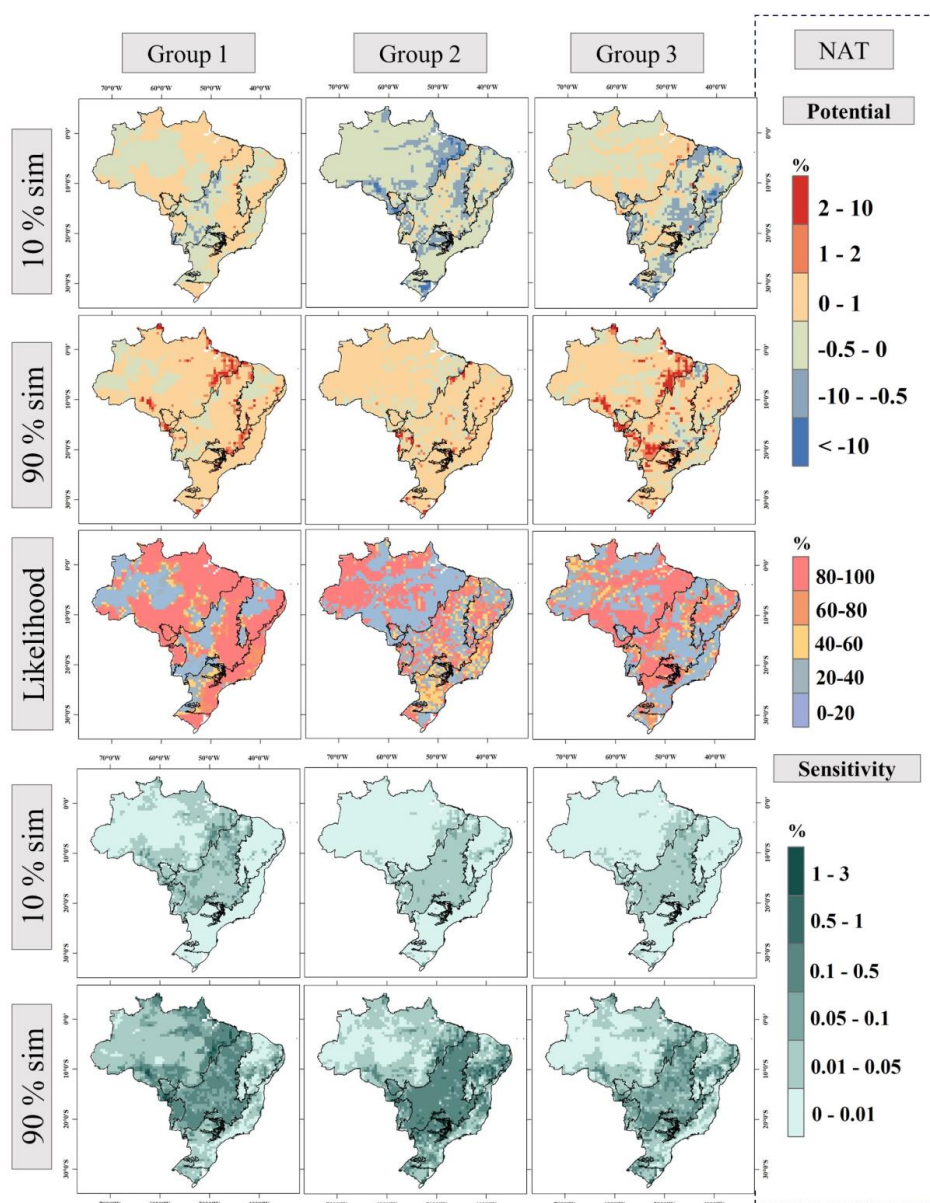
702

703

704

705

706



707

708 **Figure 9: Same as Fig. 9 but for NAT.**

709

710 Higher uncertainties were found in the potential response for NON, meaning that the range of  
 711 possible outcomes was generally larger for this category (Fig. 10). However, the likelihood  
 712 showed similar spatial variation, although unclear responses increased. Group 1 acts as a driver  
 713 of burning in 62.99% of Amazonia, a similar number when compared to NAT and ALL. The



714 main difference for this category is the magnitude of increase, which is higher at the edges and  
715 in the middle of the biome. Likewise, the sensitivity was higher, especially in the 90th  
716 percentile. The potential and sensitivity response of the Atlantic Forest was quite similar for  
717 the three categories, with 64.61% likely to have Group 1 increasing burning in the biome.  
718 Within the Cerrado, a 13.15% and 9.67% increase in areas susceptible to burning is observed  
719 compared to ALL and NAT respectively (totaling 71.45%). Unclear responses were higher and  
720 reached 9.21% of the biome. Sensitivity was higher in the northeast of the biome. For Pantanal,  
721 NON comprised 69.23% of areas likely to burn due to Group 1. An increase in unclear  
722 responses of 7.7% and 9.62% compared to ALL and NAT respectively was found (totaling  
723 13.45% of the biome). The magnitude of increase was also higher for NON. Sensitivity levels  
724 were mostly high across the biome. Within Pampas, 79.10% of the biome was considered likely  
725 to burn due to Group 1. The sensitivity was larger at the edges of the biome. The potential and  
726 sensitivity responses of Caatinga followed a similar pattern between the categories, where  
727 47.70% of the biome is likely to be susceptible to burning due to Group 1.  
728

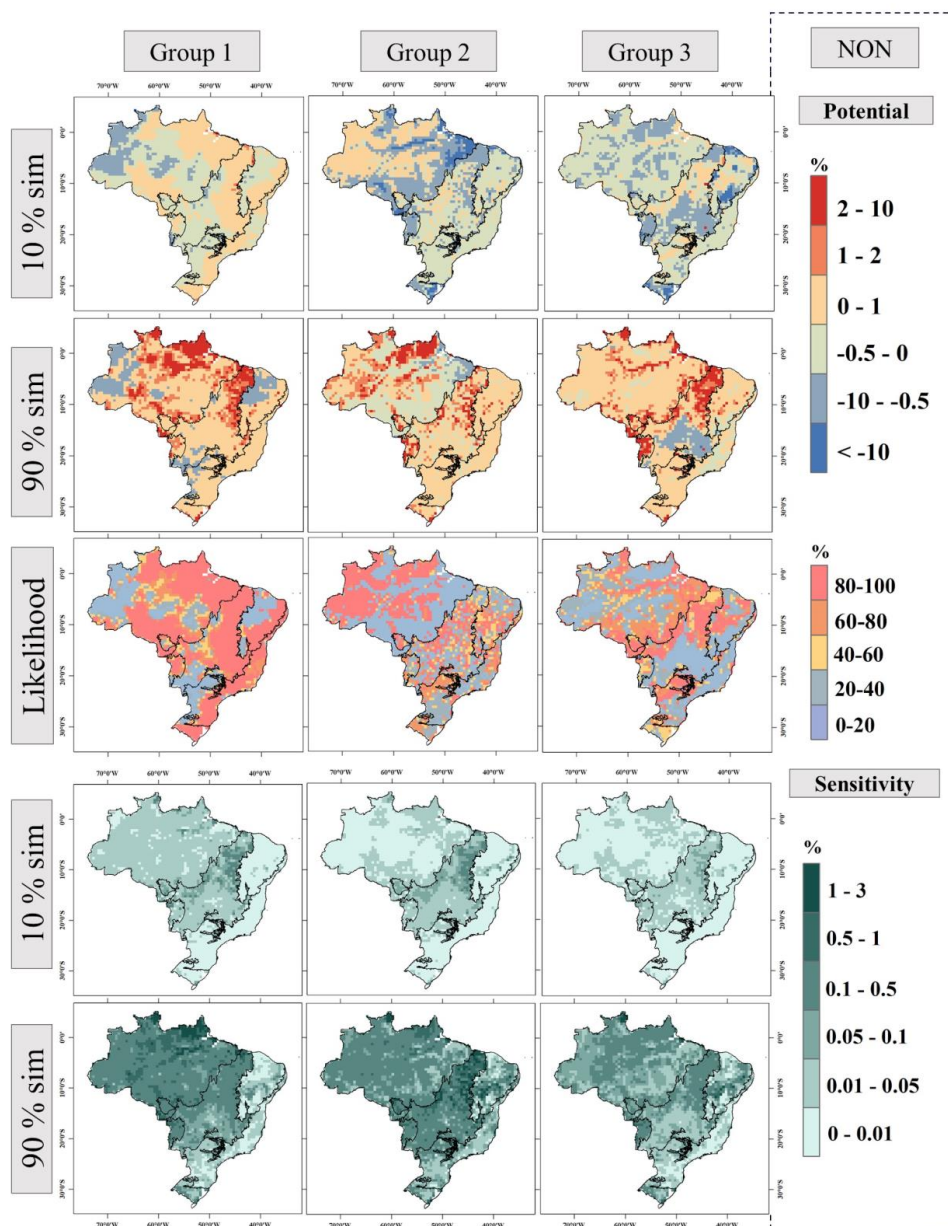
729 Similarly, the main difference for Group 2 in Amazonia was the increase, which reached up to  
730 10% in the North and middle of the biome. Most of the biome shows high sensitivity. Within  
731 the Atlantic Forest, there was a notable reduction of 30.51% in regions with unclear responses  
732 compared to the NAT, where the proportion was 11.28%. Regions likely to increase burned  
733 area due to fragmentation comprise 41.28% of the biome, an increase of 14.87% compared to  
734 NAT. Sensitivity showed a similar pattern for the three categories where regions likely to  
735 increase burning presented higher sensitivities. In Cerrado, approximately 41.54% of its area  
736 is likely susceptible to increased burning due to fragmentation, with 15.70% exhibiting unclear  
737 responses. Higher sensitivity was observed in the northeastern region of the biome. Pantanal  
738 showed a 40.38% likely increase and a significant sensitivity across the biome. Pampas patterns  
739 for potential and sensitivity responses were similar to ALL and NAT, with 49.25% of the biome  
740 likely to increase burning. However, the likelihood was comparatively lower (between 60%  
741 and 80%). For Caatinga, it is likely to increase burning in 36.39% of the biome, while the  
742 regions with unclear response reached 21.90%. Sensitivity displayed a similar pattern to ALL  
743 and NAT with higher sensitivities in the middle and northeast.  
744

745 Group 3 exhibited higher uncertainties in Amazonia between the 10th and 90th percentiles.  
746 The likelihood of increase encompasses 44.59% of the biome, while areas with unclear  
747 responses surpass ALL and NAT, comprising 10.21%. Sensitivity was also higher, especially



748 in the north of Amazonia. The Atlantic Forest showed a similar pattern compared to ALL and  
749 NAT with 38.71% of its area likely to increase and generally lower sensitivity to this group.  
750 Cerrado exhibited a marked pattern where burning in the north is likely driven by Group 3,  
751 encompassing 40.78% of the biome. These regions also exhibited higher sensitivity to minor  
752 variations in Group 3. Unclear responses were identified in 11.48% of the biome. This Group  
753 exhibited the highest level of unclear response in the Pantanal, totaling 30.77%. Meanwhile,  
754 regions with a likelihood of increased burning decreased to 25%. The sensitivity was generally  
755 high across the biome. This group also showed to be highly uncertain in Pampas, with 55.22%  
756 of the biome presenting unclear responses. The areas likely to increase burning comprised  
757 23.88% of Pampa, a reduction of 28.35% and 20.89% compared to ALL and NAT,  
758 respectively. The sensitivity was similar in the three categories with slightly higher sensitivity  
759 in the middle for NON. The Caatinga region exhibited a 35.33% portion of its area with a  
760 heightened likelihood of increased burning attributed to Group 3, displaying a similar pattern  
761 across all three categories concerning potential and sensitivity response.  
762





763  
764 **Figure 10: Same as Fig.9 but for NON.**  
765  
766  
767  
768  
769





770 **4 DISCUSSION**

771

772 **4.1 FLAME's performance in context**

773

774 Our proposed model uniquely combines two previously distinct approaches employed in fire  
775 modeling: Bayesian inference and Maximum Entropy (KELLEY et al., 2021; FERREIRA et  
776 al., 2023). This combination allows for a more comprehensive understanding of fire dynamics  
777 as it models a probability distribution rather than singular values, a departure from conventional  
778 models (e.g. HANTSON et al., 2016; RABIN et al., 2017). Notably, our approach employs  
779 Maximum Entropy to capture the most uncertain outcomes that align with our priors, reflecting  
780 the stochastic nature of real-world fires. This concept contributes to a more nuanced and  
781 realistic representation of fire behavior. We conducted our analysis by categorizing the burned  
782 area into three categories: fires in both natural and non-natural vegetation (ALL), fires reaching  
783 natural vegetation (NAT), and fires reaching non-natural vegetation (NON). This classification  
784 yielded distinct results for each category with an overall improvement across the biomes for  
785 the NAT and NON. Moreover, this approach allows us to make more targeted conclusions.  
786

787 The results demonstrate the robust performance of our model in capturing observations while  
788 providing a range of possible outcomes represented by the 10th and 90th percentiles. It is  
789 noteworthy that the model was capable of reproducing the observations in Pampa, Atlantic  
790 Forest and Caatinga, as these are areas where other methods used in previous studies have not  
791 performed well (NOGUEIRA et al. 2017, OLIVEIRA et al., 2022). Despite some level of bias  
792 in the results, even during periods of suboptimal performance, the likelihood of the  
793 observations remained consistently high, with the majority exceeding 80%. The Pantanal  
794 biome presented an exception, displaying a likelihood of 59% for the combined category  
795 (ALL), with improvement for specific categories, reaching 86% for NAT and 78% for NON.  
796 This biome encompasses a mosaic of vegetation types characterized by seasonally flooded  
797 areas which plays an important role on the fire dynamics of the region (DAMASCENO-  
798 JUNIOR et al., 2021). Fire in these areas were not included in this study due to our general  
799 approach, posing a limitation for simulation within this biome. However, our framework's  
800 adaptability means that future work could look at different explanatory variables, relationship  
801 variables and fire categorizations that could target performance in places like the Pantanal.

802



803 The MaxEnt species distribution model, which uses the same Maximum Entropy concept  
804 applied here, became quite popular in fire modeling studies (e.g., FONSECA et al., 2017;  
805 BANERJEE, 2021; FERREIRA et al., 2023). However, the MaxEnt software provides default  
806 settings, based on average values which are likely to change according to species, study region  
807 and environmental data (PHILLIPS and DUDIK, 2008). Additionally, these current settings  
808 are estimated to result in excessively complex models, potentially leading to overfitting  
809 (RADOSAVLJEVIC and ANDERSON, 2013). When employing MaxEnt, it is crucial to  
810 utilize independent evaluation data (PETERSON et al., 2011) such as that used in the present  
811 study. However, many studies assess performance by randomly partitioning occurrence data  
812 into calibration and evaluation datasets (CHEN et al., 2015; GÖLTAS et al., 2024). This  
813 approach limits the ability to obtain reliable estimates of model performance, generality, and  
814 transferability. Finally, the area under the receiver operating characteristic (ROC) curve,  
815 commonly known as AUC, is widely used as a standard method to evaluate the accuracy of  
816 MaxEnt-based models. Nonetheless, this measure does not provide information about the  
817 spatial distribution of the model's performance (LOBO et al., 2007; JIMÉNEZ-VALVERDE,  
818 2011) which also potentially masks the spatial variability of the explanatory variables  
819 contribution to the model.

820

821 Currently, global fire models incompletely reproduce the observed spatial patterns of burned  
822 area. We found that FLAME captures high burning events, albeit not with the exact magnitude  
823 observed. This ability presents an advantage compared to many global fire models. While  
824 global fire modeling provides useful information into broad-scale patterns and trends, they are  
825 mostly designed to estimate global mean burned area (HANTSON et al., 2016; BURTON and  
826 LAMPE et al., 2023). As a result, its applicability to regional scales such as the Brazilian  
827 biomes is inherently limited. Furthermore, these models are typically constructed based on  
828 assumptions regarding variable relationships, which may not hold true in all locations due to  
829 variations in environmental conditions, ecosystem dynamics, and human activities. However,  
830 Earth System Models integrate feedback mechanisms between burned areas and predictor  
831 variables, enabling the evaluation of inter-variable effects. FLAME is not designed to capture  
832 these feedbacks, underscoring the need for tailored methodologies to address specific research  
833 questions.

834

#### 835 **4.2 Burning controls across the biomes**

836



837 We combined our variables into three groups to assess their compound effect on the burned  
838 area. This is a similar approach to Kelley et al. (2019) who also used a Bayesian framework to  
839 assess drivers of global fire regimes. Nonetheless, Kelley et al. (2019) considered only linear  
840 responses which is especially challenging when considering the varying responses across the  
841 globe. Our results highlighted the spatial variability of each variable group's influence on  
842 burning within and between each biome. The potential response displayed similar spatial  
843 likelihood variation between the ALL, NAT and NON categories. However, differences were  
844 still observed, especially for the fire-dependent biomes (Cerrado and Pantanal). Overall, the  
845 uncertainties were larger for the NON category, particularly for Pampas and Pantanal.

846

847 For example, Maximum Temperature and Precipitation (Group 1) are likely drivers of burning  
848 in large portions of each biome during the fire peak, as demonstrated by the potential and  
849 sensitivity results. Our results indicate that in highly forested areas in Amazonia, climate alone  
850 does not control burning, suggesting that forests can potentially mitigate the effects of climate  
851 in burned area. These regions showed up to three times less sensitivity to minor variations of  
852 climate for NAT while ALL and NON displayed high sensitivity in the whole biome. However,  
853 natural landscapes, especially forests, are highly susceptible during extreme weather conditions  
854 (DOS REIS et al., 2021; BARBOSA et al., 2022). This suggests that projected climate change  
855 could greatly increase the risk of Amazon forest fires (FLORES et al., 2024). Moreover, non-  
856 natural vegetation in Amazonia is mainly concentrated in the arc of deforestation, reducing the  
857 samples for this category in other parts of the Amazon and potentially influencing the model's  
858 response. An opposite dynamic was found in Cerrado and Pantanal. Regions with large areas  
859 of natural vegetation were more likely to be influenced by climate. These regions were more  
860 sensitive to minor variations in climate for NON in Cerrado while the entire Pantanal displayed  
861 similar sensitivity in the three categories. This aligns with prior research showing that fires in  
862 Cerrado are linked with meteorological conditions, particularly rainfall and temperature  
863 (NOGUEIRA et al., 2017; LIBONATI et al., 2022; LI et al., 2022). Similarly, in Pantanal, the  
864 2020 fire season revealed the connections between meteorological conditions and increased  
865 burning in the biome (BARBOSA et al., 2022; LIBONATI et al. 2022b) and again during the  
866 2023 El Niño. Barbosa et al., (2022), reported that 84% of the 2020 record of fires in Pantanal  
867 occurred in natural vegetation, with a 514% increase from average within forests. Despite being  
868 a combination with land use, the precipitation and maximum temperature anomalies were  
869 particularly high in 2020, contributing to the spread of fires into fire-sensitive vegetation.

870



871 Group 2 (Edge density and Road density) encompasses variables expected to have uncertain  
872 response across the biomes. Within Cerrado, 40.63% of its area will likely decrease burned  
873 area for NAT due to Group 2. A high density of forest edges has been associated with a higher  
874 incidence of fires in forest ecosystems (ARMENTERAS et al., 2013; SILVA-JUNIOR et al.,  
875 2022). However, fragmentation can also act as a barrier to fire spread, potentially reducing fire  
876 occurrences (DRISCOLL et al., 2021). Rosan et al., (2022), revealed that in Cerrado,  
877 fragmentation correlates with a decrease in burned area fraction, while in Amazonia, it is  
878 linked to an increase in burning. Nevertheless, we found a decrease in burning where edge  
879 densities are concentrated in the Amazon. This could indicate that the edges of the Amazon are  
880 reaching a level of fragmentation that fires are impeded from spreading, considering the  
881 reduction of aboveground biomass near forest edges (NUMATA et al., 2017). However, further  
882 research is needed to test this hypothesis.

883

884 Depending on the landscape, road densities can also exhibit contrasting relationships with fires.  
885 While more fires are expected surrounding roads (ARMENTERAS et al., 2017), less fires are  
886 expected with increased density due to urbanization. The Atlantic Forest is a very fragmented  
887 biome with very high densities of natural edges and roads (Fig. 3). We found an uncertain  
888 response for NAT in 41.79% of the Atlantic Forest and only 26.41% likely to increase. Singh  
889 and Huang (2022) suggests that the fragmentation partly explains burned area variation in the  
890 Atlantic Forest where small patches are more vulnerable to fires. The majority of Caatinga is  
891 likely to decrease burning due to Group 2. However, the sensitivity was up to three times higher  
892 in the middle and northeast, which is more likely to increase. Antongiovanni et al. (2020)  
893 discussed that fires in Caatinga occur at all edge distances, although they are slightly more  
894 frequent at fragment edges. Nonetheless, the limited amount of studies across the different  
895 biomes addressing these relationships makes it harder to understand the related uncertainties.

896

897 Group 3 is likely to influence burning in 54.74% of Amazonia for NAT, particularly in the arc  
898 of deforestation. This suggests that the combination of less forest, increased pasture and more  
899 fuel (Fig. 3) increases burning in natural lands in Amazonia, corroborating previous findings  
900 (SILVEIRA et al., 2020; SILVEIRA et al., 2022). The relationship in Pantanal and Pampa  
901 showed that these variables increase burning in 32.69% (NAT) and 25% in Pantanal and  
902 44.78% (NAT) and 23.88% (NON) for Pampas. The regions with unclear responses were the  
903 highest for NON, 30.77% of Pantanal and 55.22% of Pampa. These biomes are characterized  
904 by lower forest and pasture cover (Fig. 3) with fires and cattle ranching mainly linked to



905 grasslands (BARBOSA et al., 2022; FIDELIS et al., 2022; CHIARAVALLOTTI et al., 2023).  
906 Thus, incorporating grassland cover in the model will likely reveal further relationships  
907 between burned area and LULC in these biomes. Caatinga showed increased sensitivity where  
908 Group 3 is likely to increase burning, matching the area of influence of Group 2. This area is  
909 associated with low forest cover and soil carbon and moderate pasture cover. Araújo et al.  
910 (2012), observed that due to the intermittent and scattered characteristics of cattle ranching in  
911 the Caatinga, fires tend to occur mainly in natural vegetation, characterized by large cover of  
912 savanna vegetation. Although our study provides a general overview of burning dynamics in  
913 the biomes, targeting variables is highly recommended in future studies, especially where fires  
914 are poorly understood as in Caatinga.

#### 915 **4.3 FLAME potentialities**

916 Further developments are recommended to improve FLAME's capabilities. Exploring and  
917 incorporating better-informed and additional priors may constrain the variables' response  
918 uncertainties. Utilizing alternative metrics to assess drivers, particularly those tailored to  
919 specific biomes, could offer a more nuanced understanding of the influencing factors. It could  
920 also help improve biases in biomes such as the Pantanal. Customizing variable selection based  
921 on biome characteristics would also contribute to a more biome-focused and contextually  
922 relevant analysis. Consideration of different fire categories show how the model could be used  
923 in further research. For instance, a more detailed stratification could involve categorizing fires  
924 into distinct groups such as forest, agricultural, and deforestation fires. While deforestation data  
925 was not incorporated in this study, efforts should be made to integrate this valuable information  
926 where possible. Furthermore, accounting for the varying proportions of natural and non-natural  
927 lands within each pixel, as demonstrated in this study, provides a more accurate landscape  
928 representation. This contributes to improved simulations where these areas are very small. In  
929 addition, finer grids and the subdivision of the biomes may uncover local processes, though  
930 eventually fire spread between fine-scales would need to be considered. This could be crucial  
931 for understanding localized patterns and improving the model's predictive capabilities. Perilous  
932 modeling attempts often parameterize on a large regional basis. However, our approach allows  
933 for optimization on much smaller areas while still quantifying the confidence in the analysis.  
934 FLAME is flexible enough to be used in various locations and, through targeted benchmarking,  
935 holds the potential to evaluate extreme fires, inter-annual and seasonal variability of fires,  
936 project future fires, and simulate other hazards. With appropriate adaptations and



937 enhancements, FLAME has the potential to evolve into a robust model capable of simulating  
938 terrestrial impacts effectively.

939

## 940 **5 FINAL CONSIDERATIONS**

941

942 The self-reinforcing cycle between fires and climate change makes it fundamental to improve  
943 fire simulations. An understanding of what drives fires is essential for devising mitigation and  
944 adaptation strategies. However, it can be particularly challenging due to the intricate interplay  
945 of various factors, especially in a diverse country like Brazil. We propose a novel approach for  
946 simulating burned area in the Brazilian biomes that keeps assumptions at a minimum whilst  
947 quantifying uncertainties. The model performs well in all biomes, and enables the assessment  
948 of fire categories and the grouped effect of variables. Furthermore, conventional modeling  
949 efforts often parameterize at a large scale. FLAME enables optimization in smaller areas while  
950 still providing a means to quantify confidence in the analysis.

951

952 Climate is an important factor in burned area in all biomes. Despite several studies showing  
953 this relationship, climate-related uncertainties had not been extensively quantified, a gap this  
954 research fulfills. Groups 2 (road and edge densities) and 3 (forest, pasture and soil carbon) and  
955 the NON category showed the highest uncertainties among the responses. This highlights the  
956 challenge in modeling human-related factors. Pantanal, Cerrado, and Amazonia showed higher  
957 sensitivity to minor variations in the variables. It is important to note that sensitivity is more  
958 important where burning is already high, which is the case in these biomes (ALENCAR et al.,  
959 2022). None of the groups drive huge changes in burned area in the Atlantic Forest, though as  
960 it is fire-sensitive, it still can have a large impact. Uncertain responses compound the  
961 complexity of burned area drivers as different variables interact uniquely within each biome.  
962 The same vegetation type may show contrasting responses to the same drivers in different  
963 locations. Therefore, no universal fire management policies will fit the whole country. In  
964 particular, Caatinga, Atlantic Forest and Pampa require further investigation. Emphasizing  
965 regional-scale analysis is crucial for decision-makers and fire management strategies, enabling  
966 more informed and effective prevention of fires.

967

## 968 **CODE AVAILABILITY**

969

970 FLAME 1.0 model code is available at <https://doi.org/10.5281/zenodo.13367375> (Barbosa et  
971 al., 2024a).



972

973 **DATA AVAILABILITY**

974

975 The data supporting this study is available at the Zenodo repository:

976 <https://doi.org/10.5281/zenodo.11491125> (Barbosa et al, 2024b).

977

978 **AUTHOR CONTRIBUTIONS**

979

980 **Conceptualization:** MLFB, DIK, CAB, LOA

981

982 **Data Curation:** MLFB, DIK, AB

983

984 **Formal Analysis:** MLFB, DIK

985

986 **Methodology:** MLFB, DIK, CAB

987

988 **Resources/Software:** MLFB, DIK, CAB

989

990 **Visualization:** MLFB

991

992 **Funding acquisition:** MLFB, LOA

993

994 **Supervision:** LOA, DIK, CAB

995

996 **Resources:** LOA, DIK, CAB

997

998 **Writing – Original Draft Preparation:** MLFB

999

1000 **Writing – Review & Editing:** MLFB, IJMF, RMV, AB, PGM

1001

1002 All co-authors approved the draft

1003

1004 **COMPETING INTERESTS**

1005

1006 The authors declare that they have no conflict of interest.

1007

1008 **FUNDING ACKNOWLEDGMENTS**

1009 DIK was supported by the Natural Environment Research Council as part of the LTSM2

1010 TerraFIRMA project and NC-International programme [NE/X006247/1] delivering National

1011 Capability. This work and its contributors (CAB, AB) were funded by the Met Office Climate

1012 Science for Service Partnership (CSSP) Brazil project which is supported by the Department

1013 for Science, Innovation & Technology (DSIT). LOA acknowledges support by the São Paulo

1014 Research Foundation (FAPESP) (projects: 2021/07660-2 and 2020/16457-3) and by the

1015 National Council for Scientific and Technological Development (CNPq) project 409531/2021-

1016 9 and productivity scholarship (process: 314473/2020-3). MLFB and IJMF were supported by

1017 the Coordination for the Improvement of Higher Education Personnel (CAPES), Finance Code

1018 001. MLFB and PGM acknowledges support by the São Paulo Research Foundation (FAPESP)





1019 (project: 2021/11940-0). RMV thanks the São Paulo Research Foundation (FAPESP) for grants  
1020 2020/06470-2 and 2022/13322-5.

1021

## 1022 ACKNOWLEDGMENTS

1023 Eleanor Burke (UK Met Office) for original JULES-ES simulations.

1024 Tristan Quaife (University of Reading) for supervisor support.

1025 Eddy Robertson (UK Met Office) for support and discussion on this research.

1026

## 1027 REFERENCES

1028 ABRIL-PLA, O.; ANDREANI, V.; CARROLL, C.; DONG, L.; FONNESBECK, C. J.;  
1029 KOCHUROV, M.; KUMAR, R.; LAO, J.; LUHMANN, C. C.; MARTIN, O. A.; OSTHEGE,  
1030 M.; VIEIRA, R.; WIECKI, T.; ZINKOV, R. **PyMC: A Modern and Comprehensive**  
1031 **Probabilistic Programming Framework in Python. Computer Science**, v.9, p. e1516, 2023.

1032 ALENCAR, A.A.; ARRUDA, V.L.; SILVA, W.V.D.; CONCIANI, D.E.; COSTA, D.P.;  
1033 CRUSCO, N.; DUVERGER, S.G.; FERREIRA, N.C.; FRANCA-ROCHA, W.; HASENACK,  
1034 H. AND MARTENEXEN, L.F.M. Long-term landsat-based monthly burned area dataset for  
1035 the Brazilian biomes using deep learning. **Remote Sensing**, v.14, p.2510, 2022.

1036 ANDELA, N., MORTON, D.C., GIGLIO, L., CHEN, Y., VAN DER WERF, G.R.,  
1037 KASIBHATLA, P.S., DEFRIES, R.S., COLLATZ, G.J., HANTSON, S., KLOSTER, S. AND  
1038 BACHELET, D. A human-driven decline in global burned area. *Science*, v.356, p.1356-1362,  
1039 2017.

1040 ANTONGIOVANNI, M.; VENTICINQUE, E.M.; MATSUMOTO, M.; FONSECA, C.R.  
1041 Chronic anthropogenic disturbance on Caatinga dry forest fragments. **Journal of Applied**  
1042 **Ecology**, v. 57, p.2064-2074, 2020.

1043 ARAGAO, L.E.O.; MALHI, Y.; BARBIER, N.; LIMA, A.; SHIMABUKURO, Y.;  
1044 ANDERSON, L.; SAATCHI, S. Interactions between rainfall, deforestation and fires during  
1045 recent years in the Brazilian Amazonia. **Philosophical Transactions of the Royal Society B:**  
1046 **Biological Sciences**, v.363, n.1498, p.1779-1785, 2008.

1047 ARMENTERAS, D.; GONZÁLEZ, T.M; RETANA, J. Forest fragmentation and edge  
1048 influence on fire occurrence and intensity under different management types in Amazon  
1049 forests. **Biological Conservation**, v.159, p.73-79, 2013.

1050 ARMENTERAS, D.; BARRETO, J.S.; TABOR, K.; MOLOWNY-HORAS, R.; RETANA, J.  
1051 Changing patterns of fire occurrence in proximity to forest edges, roads and rivers between  
1052 NW Amazonian countries. **Biogeosciences**, v.14, p.2755-2765, 2017.

1053 BANERJEE, P., 2021. Maximum entropy-based forest fire likelihood mapping: analysing the  
1054 trends, distribution, and drivers of forest fires in Sikkim Himalaya. *Scandinavian Journal of*  
1055 *Forest Research*, 36(4), pp.275-288.





- 1056 BARBOSA, M.L.F., HADDAD, I., DA SILVA NASCIMENTO, A.L., MAXIMO DA SILVA,  
1057 G., MOURA DA VEIGA, R., HOFFMANN, T.B., ROSANE DE SOUZA, A., DALAGNOL,  
1058 R., SUSIN STREHER, A., SOUZA PEREIRA, F.R. AND OLIVEIRA E CRUZ DE  
1059 ARAGÃO, L.E., 2022. Compound impact of land use and extreme climate on the 2020 fire  
1060 record of the Brazilian Pantanal. *Global Ecology and Biogeography*, 31(10), pp.1960-1975.
- 1061 BARBOSA, M.L.F, KELLEY, D., BURTON, C. & ANDERSON, L. (2024a). malu-  
1062 barbosa/FLAME: FLAME 1.0: Fogo local analisado pela Máxima Entropia (v0.1). Zenodo.  
1063 <https://doi.org/10.5281/zenodo.13367375>.
- 1064 BARBOSA, M.L.F, KELLEY, D., BRADLEY, A., & BURTON, C. (2024b). FLAME 1.0: a  
1065 novel approach for modelling burned area in the Brazilian biomes using the Maximum Entropy  
1066 concept - Input Data [Data set]. Zenodo. <https://doi.org/10.5281/zenodo.11491125>.
- 1067 BURTON C, BETTS R, CARDOSO M, FELDPAUSCH TR, HARPER A, JONES CD,  
1068 KELLEY DI, ROBERTSON E, WILTSHIRE A. Representation of fire, land-use change and  
1069 vegetation dynamics in the Joint UK Land Environment Simulator vn4. 9 (JULES).  
1070 *Geoscientific Model Development*. 2019 Jan 9;12(1):179-93.
- 1071 BURTON C, KELLEY DI, JONES CD, BETTS RA, CARDOSO M, ANDERSON L. South  
1072 American fires and their impacts on ecosystems increase with continued emissions. *Climate  
1073 Resilience and Sustainability*. 2022 Feb;1(1):e8.
- 1074 BURTON, C.; LAMPE, S.; KELLEY, D.; THIERY, W.; HANTSON, S.; CHRISTIDIS, N.;  
1075 GUDMUNDSSON, L.; FORREST, M.; BURKE, E.; CHANG, J.; HUANG, H. Global burned  
1076 area increasingly explained by climate change. **Preprint** at <https://doi.org/10.21203/rs.3>.  
1077 2023.
- 1078 CAMPANHARO, W.A., LOPES, A.P., ANDERSON, L.O., DA SILVA, T.F. AND  
1079 ARAGÃO, L.E., 2019. Translating fire impacts in Southwestern Amazonia into economic  
1080 costs. *Remote Sensing*, 11(7), p.764.
- 1081 CANO-CRESPO, A.; OLIVEIRA, P. J.; BOIT, A.; CARDOSO, M.; THONICKE, K. Forest  
1082 edge burning in the Brazilian Amazon promoted by escaping fires from managed pastures.  
1083 **Journal of Geophysical Research: Biogeosciences**, v.120, p.2095-2107, 2015.
- 1084 CECIL, D.J. **LIS/OTD 0.5 degree high resolution monthly climatology (HRMC)**.  
1085 Washington: NASA, 2006.
- 1086 CHEN, F.; DU, Y.; NIU, S.; ZHAO, J. Modeling forest lightning fire occurrence in the  
1087 Daxinganling Mountains of Northeastern China with MAXENT. **Forests**, v.6, p.1422-1438,  
1088 2015.
- 1089 CHEN, X.; DIMITROV, N.B.; MEYERS, L.A. Uncertainty analysis of species distribution  
1090 models. *PloS One*, v.14, e0214190, 2019.



- 1091 CHIARAVALLOTI, R.M.; TOMAS, W.M.; AKRE, T.; MORATO, R.G.; CAMILO, A.R.;  
1092 GIORDANO, A.J.; LEIMGRUBER, P. Achieving conservation through cattle ranching: the  
1093 case of the Brazilian Pantanal. **Conservation Science and Practice**, 2023.
- 1094 DOS REIS, M.; DE ALENCASTRO GRAÇA, P.M.L.; YANAI, A.M.; RAMOS, C.J.P.;  
1095 FEARNSIDE, P.M. Forest fires and deforestation in the central Amazon: effects of landscape  
1096 and climate on spatial and temporal dynamics. **Journal of Environmental Management**,  
1097 v.288, p.112310, 2021.
- 1098 DOS SANTOS, A.C.; DA ROCHA MONTENEGRO, S.; FERREIRA, M.C.; BARRADAS,  
1099 A.C.S.; SCHMIDT, I.B. Managing fires in a changing world: fuel and weather determine fire  
1100 behavior and safety in the neotropical savannas. **Journal of Environmental Management**,  
1101 v.289, p.112508, 2021.
- 1102 DRISCOLL, D.A.; ARMENTERAS, D.; BENNETT, A.F.; BROTONS, L.; CLARKE, M.F.;  
1103 DOHERTY, T.S.; HASLEM, A.; KELLY, L.T.; SATO, C.F.; SITTERS, H.; AQUILUÉ, N.  
1104 How fire interacts with habitat loss and fragmentation. **Biological Reviews**, v.96, p.976-998,  
1105 2021.
- 1106 ELITH, J.; PHILLIPS, S.J.; HASTIE, T.; DUDÍK, M.; CHEE, Y.E.; YATES, C.J. A statistical  
1107 explanation of MaxEnt for ecologists. *Diversity and Distributions*, v.17, p.43-57, 2011.
- 1108 FERREIRA, I.J.; CAMPANHARO, W.A.; BARBOSA, M.L.; SILVA, S.S.D.; SELAYA, G.;  
1109 ARAGÃO, L.E.; ANDERSON, L.O. Assessment of fire hazard in Southwestern Amazon.  
1110 *Frontiers in Forests and Global Change*, v.6, p.1107417, 2023.
- 1111 FIDELIS, A.; SCHMIDT, I.B.; FURQUIM, F.F.; OVERBECK, G.E. Burning in the Pampa  
1112 and Cerrado in Brazil. **Global Application of Prescribed Fire**, p.38, 2022.
- 1113 FLORES, B.M.; MONTOYA, E.; SAKSCHEWSKI, B.; NASCIMENTO, N.; STAAL, A.;  
1114 BETTS, R.A.; LEVIS, C.; LAPOLA, D.M.; ESQUÍVEL-MUELBERT, A.; JAKOVAC, C.;  
1115 NOBRE, C.A. Critical transitions in the Amazon Forest system. **Nature**, v.626, p.555-564,  
1116 2024.
- 1117 FONSECA, M.G., ANDERSON, L.O., ARAI, E., SHIMABUKURO, Y.E., XAUD, H.A.,  
1118 XAUD, M.R., MADANI, N., WAGNER, F.H. AND ARAGÃO, L.E. Climatic and  
1119 anthropogenic drivers of northern Amazon fires during the 2015–2016 El Niño event.  
1120 *Ecological applications*, v.27, p.2514-2527, 2017.
- 1121 FONSECA, M.G., ALVES, L.M., AGUIAR, A.P.D., ARAI, E., ANDERSON, L.O., ROSAN,  
1122 T.M., SHIMABUKURO, Y.E. AND DE ARAGÃO, L.E.O.E.C. Effects of climate and land-  
1123 use change scenarios on fire probability during the 21st century in the Brazilian Amazon.  
1124 *Global change biology*, v.25, p.2931-2946, 2019.
- 1125 FORKEL, M., ANDELA, N., HARRISON, S.P., LASSLOP, G., VAN MARLE, M.,  
1126 CHUVIECO, E., DORIGO, W., FORREST, M., HANTSON, S., HEIL, A., LI, F. Emergent



- 1127 relationships with respect to burned area in global satellite observations and fire-enabled  
1128 vegetation models. *Biogeosciences*. 2019 Jan 11;16(1):57-76.
- 1129 FRIELER, K. et al. Scenario set-up and forcing data for impact model evaluation and impact  
1130 attribution within the third round of the Inter-Sectoral Model Intercomparison Project  
1131 (ISIMIP3a). *EGUsphere* 2023, 1–83 (2023).
- 1132 GELMAN, ANDREW; CARLIN, JOHN B.; STERN, HAL S.; DUNSON, DAVID B.;  
1133 VEHTARI, AKI; RUBIN, DONALD B. (2013). *Bayesian Data Analysis, Third Edition*.  
1134 Chapman and Hall/CRC. ISBN 978-1-4398-4095-5.
- 1135 GIGLIO, L., BOSCHETTI, L., ROY, D. P., HUMBER, M. L., AND JUSTICE, C. O. The  
1136 Collection 6 MODIS burned area mapping algorithm and product, *Remote Sens. Environ.*, 217,  
1137 72–85, 2018.
- 1138 GÖLTAS, M.; AYBERK, H.; KÜCÜK, O. Forest fire occurrence modeling in Southwest  
1139 Turkey using MaxEnt machine learning technique. ***iForest-Biogeosciences and Forestry***,  
1140 v.17, p.10, 2024.
- 1141 HANTSON, S.; ARNETH, A.; HARRISON, S.P.; KELLEY, D.I.; PRENTICE, I.C.; RABIN,  
1142 S.S.; ARCHIBALD, S.; MOUILLOT, F.; ARNOLD, S.R.; ARTAXO, P.; BACHELET, D.  
1143 The status and challenge of global fire modelling. *Biogeosciences*, v.13, p.3359-75, 2016.
- 1144 HANTSON, S., KELLEY, D. I., ARNETH, A., HARRISON, S. P., ARCHIBALD, S.,  
1145 BACHELET, D., FORREST, M., HICKLER, T., LASSLOP, G., LI, F., MANGEON, S.,  
1146 MELTON, J. R., NIERADZIK, L., RABIN, S. S., COLIN PRENTICE, I., SHEEHAN, T.,  
1147 SITCH, S., TECKENTRUP, L., VOULGARAKIS, A. AND YUE, C.: Quantitative assessment  
1148 of fire and vegetation properties in historical simulations with fire-enabled vegetation models  
1149 from the FireModel Intercomparison Project, *Geoscientific Model Development Discussions* ,  
1150 2020.
- 1151 HARDESTY, J., MYERS, R. AND FULKS, W. 2005, January. Fire, ecosystems, and people:  
1152 a preliminary assessment of fire as a global conservation issue. In *The George Wright Forum*  
1153 (Vol. 22, No. 4, pp. 78-87). George Wright Society.
- 1154 HESSELBARTH, M. H. K.; SCIAINI, M.; NOWOSAD, J.; HANSS, S.; GRAHAM, L. J.;  
1155 HOLLISTER, J.; WITH, K. A.; PRIVÉ, F.; PROJECT NAYUKI; STRIMAS-MACKEY, M.  
1156 **Landscape Metrics for Categorical Map Patterns**, 2024. Available at: [https://cran.r-](https://cran.r-project.org/web/packages/landscapemetrics/landscapemetrics.pdf)  
1157 [project.org/web/packages/landscapemetrics/landscapemetrics.pdf](https://cran.r-project.org/web/packages/landscapemetrics/landscapemetrics.pdf).
- 1158 HOFFMAN, M.D.; GELMAN, A. The No-U-Turn sampler: adaptively setting path lengths in  
1159 Hamiltonian Monte Carlo. ***Journal of Machine Learning Research***, v.15, p.1593-623, 2014.
- 1160 JAYNES, E.T. Information theory and statistical mechanics. *Physical Review*, v.106, p.620–  
1161 630, 1957.



- 1162 JIMÉNEZ-VALVERDE, A. Insights into the area under the receiver operating characteristic  
1163 curve (AUC) as a discrimination measure in species distribution modelling. **Global Ecology  
1164 and Biogeography**, v.21, p.498-507, 2011.
- 1165 JING, W.A.N., QI, G.J., JUN, M.A., REN, Y., RUI, W.A.N.G. AND MCKIRDY, S., 2020.  
1166 Predicting the potential geographic distribution of *Bactrocera bryoniae* and *Bactrocera  
1167 neohumeralis* (Diptera: Tephritidae) in China using MaxEnt ecological niche modeling. *Journal  
1168 of Integrative Agriculture*, 19(8), pp.2072-2082.
- 1169 KRAWCHUK, M. A.; MORITZ, M. A. Burning issues: statistical analyses of global fire data  
1170 to inform assessments of environmental change. *Environmetrics*, v.25, p.472–481, 2014.
- 1171 KELLEY, D.I., HARRISON, S.P. Enhanced Australian carbon sink despite increased wildfire  
1172 during the 21st century. *Environmental Research Letters*, v.9, p.104015, 2014.
- 1173 KELLEY, D.I.; BISTINAS, I.; WHITLEY, R.; BURTON, C.; MARTHEWS, T.R.; DONG, N.  
1174 How contemporary bioclimatic and human controls change global fire regimes. **Nature  
1175 Climate Change**, v.9, p.690-696, 2019.
- 1176 KELLEY, D.I.; BURTON, C.; HUNTINGFORD, C.; BROWN, M.A.; WHITLEY, R.; DONG,  
1177 N. Low meteorological influence found in 2019 Amazonia fires. **Biogeosciences Discussions**,  
1178 p.1-17, 2021.
- 1179 LAPLACE PS. Analytical probability theory. Courcier; 1820.
- 1180 LI, B., LIU, B., GUO, K., LI, C. AND WANG, B., 2019. Application of a maximum entropy  
1181 model for mineral prospectivity maps. *Minerals*, 9(9), p.556.
- 1182 LI, S.; RIFAI, S.; ANDERSON, L. O.; SPARROW, S. Identifying local-scale meteorological  
1183 conditions favorable to large fires in Brazil. **Climate Resilience and Sustainability**, v.1, e11,  
1184 2022.
- 1185 LIBONATI, R.; GEIRINHAS, J.L.; SILVA, P.S.; MONTEIRO DOS SANTOS, D.;  
1186 RODRIGUES, J.A.; RUSSO, A.; PERES, L.F.; NARCIZO, L.; GOMES, M.E.; RODRIGUES,  
1187 A.P.; DACAMARA, C.C. Drought–heatwave nexus in Brazil and related impacts on health  
1188 and fires: a comprehensive review. **Annals of the New York Academy of Sciences**, v.1517,  
1189 p.44-62, 2022.
- 1190 LIBONATI, R.; GEIRINHAS, J. L.; SILVA, P. S.; RUSSO, A.; RODRIGUES, J. A.; BELÉM,  
1191 L.B.C.; NOGUEIRA, J.; ROQUE, F.O.; DACAMARA, C.C.; NUNES, A. M. B., MARENGO,  
1192 J. A.; TRIGO, R. M. Assessing the role of compound drought and heatwave events on  
1193 unprecedented 2020 wildfires in the Pantanal. **Environmental Research Letters**, v.17,  
1194 p.015005, 2022b.



- 1195 LOBO, J.M.; JIMÉNEZ-VALVERDE, A.; REAL, R. AUC: a misleading measure of the  
1196 performance of predictive distribution models. **Global Ecology and Biogeography**, v.17,  
1197 p.145-151, 2008.
- 1198 MAPBIOMAS PROJECT. **Coleção 7 da série anual de mapas de cobertura e uso da terra**  
1199 **do Brasil**. 2022. Available at: <https://brasil.mapbiomas.org/downloads/>.
- 1200 MAPBIOMAS FOGO. Coleção 2 do mapeamento das cicatrizes de fogo do Brasil (1985-  
1201 2022). 2023. Available at: [https://brasil.mapbiomas.org/wp-](https://brasil.mapbiomas.org/wp-content/uploads/sites/4/2023/08/ATBD_-_MapBiomias_Fogo_-_Colecao_2.pdf)  
1202 [content/uploads/sites/4/2023/08/ATBD - MapBiomias Fogo - Colecao\\_2.pdf](https://brasil.mapbiomas.org/wp-content/uploads/sites/4/2023/08/ATBD_-_MapBiomias_Fogo_-_Colecao_2.pdf).
- 1203 MATHISON C, BURKE E, HARTLEY AJ, KELLEY DI, BURTON C, ROBERTSON E,  
1204 GEDNEY N, WILLIAMS K, WILTSHIRE A, ELLIS RJ, SELLAR AA. Description and  
1205 evaluation of the JULES-ES set-up for ISIMIP2b. *Geoscientific Model Development*. 2023 Jul  
1206 27;16(14):4249-64.
- 1207 MEIJER, J.R.; HUIJBREGTS, M.A.J.; SCHOTTEN, C.G.J.; SCHIPPER, A.M. Global  
1208 patterns of current and future road infrastructure. **Environmental Research Letters**, v.13,  
1209 e064006, 2018.
- 1210 MENEZES, L.S.; DE OLIVEIRA, A.M.; SANTOS, F.L.; RUSSO, A.; DE SOUZA, R.A.;  
1211 ROQUE, F.O.; LIBONATI, R. Lightning patterns in the Pantanal: untangling natural and  
1212 anthropogenic-induced wildfires. *Science of the Total Environment*, v.820, p.153021, 2022.
- 1213 MET OFFICE. **Iris: a powerful, format-agnostic, and community-driven Python package**  
1214 **for analysing and visualising Earth science data, v3.6, 2010 – 2023**. Available at:  
1215 <http://scitools.org.uk/>.
- 1216 NOGUEIRA, J.M.; RAMBAL, S.; BARBOSA, J.P.R.; MOUILLOT, F. Spatial pattern of the  
1217 seasonal drought/burned area relationship across Brazilian biomes: sensitivity to drought  
1218 metrics and global remote-sensing fire products. **Climate**, v.5, p.42, 2017.
- 1219 NUMATA, I.; SILVA, S.S.; COCHRANE, M.A.; D'OLIVEIRA, M.V. Fire and edge effects  
1220 in a fragmented tropical forest landscape in the southwestern Amazon. **Forest Ecology and**  
1221 **Management**, v.401, p.135-146, 2017.
- 1222 OLIVEIRA, U.; SOARES-FILHO, B.; BUSTAMANTE, M.; GOMES, L.; OMETTO, J.P.;  
1223 RAJÃO, R. Determinants of fire impact in the Brazilian biomes. **Frontiers in Forests and**  
1224 **Global Change**, v.5, p.735017, 2022.
- 1225 PENFIELD JUNIOR, P. Principle of maximum entropy: simple form. Massachusetts:  
1226 Massachusetts Institute of Technology, 2003.
- 1227 PETERSON, A.T.; SOBERON, J.; PEARSON, R.G.; ANDERSON, R.P.; MARTINEZ-  
1228 MEYER, E.; NAKAMURA, M.; ARAUJO, M.B. **Ecological niches and geographic**  
1229 **distributions**. Princeton: Princeton University Press, 2011.



- 1230 PHILLIPS, S.J., ANDERSON, R.P. AND SCHAPIRE, R.E. Maximum entropy modeling of  
1231 species geographic distributions. *Ecological modelling*, 190:231-259, 2006.
- 1232 PHILLIPS, S.J.; DUDIK, M. Modeling of species distributions with Maxent: new extensions  
1233 and a comprehensive evaluation. **Ecography**, v.31, p.161–175, 2008.
- 1234 RABIN, S. S. ; MELTON, J. R. ; LASSLOP, G. ; BACHELET, D. ; FORREST, M. ;  
1235 HANTSON, S. ; KAPLAN, J. O. ; LI, F. ; MANGEON, S. ; WARD, D. S. ; YUE, C. The Fire  
1236 Modeling Intercomparison Project (FireMIP), phase 1: experimental and analytical protocols  
1237 with detailed model descriptions. **Geoscientific Model Development**. v.10, p.1175-97, 2017.
- 1238 RADOSAVLJEVIC, A.; ANDERSON, R.P. Making better Maxent models of species  
1239 distributions: complexity, overfitting and evaluation. **Journal of Biogeography**, v.41, p.629–  
1240 643, 2013.
- 1241 ROSAN, T.M.; SITCH, S.; MERCADO, L.M.; HEINRICH, V.; FRIEDLINGSTEIN, P.;  
1242 ARAGÃO, L.E. Fragmentation-driven divergent trends in burned area in Amazonia and  
1243 Cerrado. **Frontiers in Forests and Global Change**, v.5, p.801408, 2022.
- 1244 SILVA JUNIOR, C.H.; BUNA, A.T.; BEZERRA, D.S.; COSTA JR, O.S.; SANTOS, A.L.;  
1245 BASSON, L.O.; SANTOS, A.L.; ALVARADO, S.T.; ALMEIDA, C.T.; FREIRE, A.T.;  
1246 ROUSSEAU, G.X. Forest fragmentation and fires in the eastern Brazilian Amazon–Maranhão  
1247 State, Brazil. *Fire*, v.5, p.77, 2022.
- 1248 SILVEIRA, M.V., PETRI, C.A., BROGGIO, I.S., CHAGAS, G.O., MACUL, M.S., LEITE,  
1249 C.C., FERRARI, E.M., AMIM, C.G., FREITAS, A.L., MOTTA, A.Z. AND CARVALHO,  
1250 L.M., 2020. Drivers of fire anomalies in the Brazilian Amazon: Lessons learned from the 2019  
1251 fire crisis. *Land*, 9(12), p.516.
- 1252 SILVEIRA, M.V.; SILVA-JUNIOR, C.H.; ANDERSON, L.O.; ARAGÃO, L.E. Amazon fires  
1253 in the 21st century: the year of 2020 in evidence. **Global Ecology and Biogeography**, v.31,  
1254 p.2026-2040, 2022.
- 1255 SINGH, M.; HUANG, Z. Analysis of forest fire dynamics, distribution and main drivers in the  
1256 Atlantic Forest. **Sustainability**, v.14, p.992, 2022.
- 1257 SPEARMAN, C. The proof and measurement of association between two things. In: JENKINS,  
1258 J.J.; PATERSON, D.G. (Ed.). **Studies in individual differences: the search for intelligence**.  
1259 [S.I.]: Appleton Century Crofts, 1961. p.45-58.
- 1260 UNITED NATIONS ENVIRONMENT PROGRAMME (UNEP). Spreading like wildfire: the  
1261 rising threat of extraordinary landscape fires. 2022. Available at:  
1262 [https://www.unep.org/resources/report/spreading-wildfire-rising-threat-extraordinary-](https://www.unep.org/resources/report/spreading-wildfire-rising-threat-extraordinary-landscape-fires)  
1263 [landscape-fires](https://www.unep.org/resources/report/spreading-wildfire-rising-threat-extraordinary-landscape-fires).



1264 VOLKHOLZ, J.; LANGE, S.; GEIGER, T. ISIMIP3a population input data (v1.2). **ISIMIP**  
1265 **Repository.**

1266 WILTSHIRE AJ, BURKE EJ, CHADBURN SE, JONES CD, COX PM, DAVIES-  
1267 BARNARD T, FRIEDLINGSTEIN P, HARPER AB, LIDDICOAT S, SITCH S, ZAEHLE S.  
1268 JULES-CN: a coupled terrestrial carbon–nitrogen scheme (JULES vn5. 1). Geoscientific  
1269 Model Development. 2021 Apr 27;14(4):2161-86.

1270 WU, Y., LI, S., XU, R., CHEN, G., YUE, X., YU, P., YE, T., WEN, B., COELHO, M.D.S.Z.S.,  
1271 SALDIVA, P.H.N. AND GUO, Y., 2023. Wildfire-related PM2. 5 and health economic loss of  
1272 mortality in Brazil. Environment International, 174, p.107906.

1273 ZACHARAKIS, I., TSIHRINTZIS, V.A. Environmental Forest fire danger rating systems and  
1274 indices around the globe: a review. Land, v.12, p.194, 2023.

1275

1276

1277

1278

1279

1280

1281

1282